



# RESEARCH MEMORANDUM

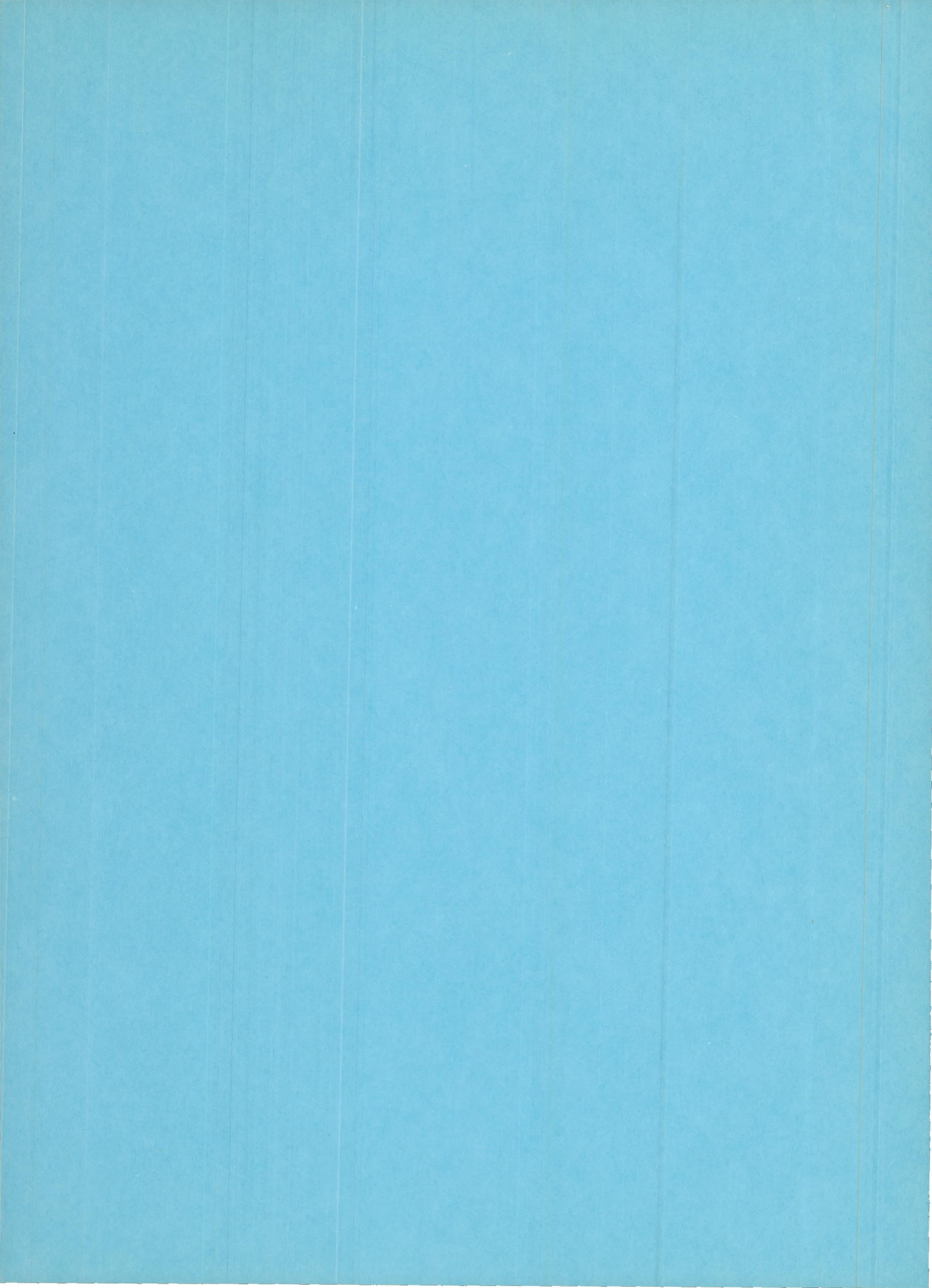
EFFECTS OF VARIATIONS IN COMBUSTION-CHAMBER  
CONFIGURATION ON IGNITION DELAY IN A 50-  
POUND-THRUST ROCKET

By Dezso J. Ladanyi

Lewis Flight Propulsion Laboratory  
Cleveland, Ohio

NATIONAL ADVISORY COMMITTEE  
FOR AERONAUTICS  
WASHINGTON

October 5, 1956  
Declassified September 17, 1958



NATIONAL ADVISORY COMMITTEE FOR AERONAUTICS

RESEARCH MEMORANDUM

EFFECTS OF VARIATIONS IN COMBUSTION-CHAMBER CONFIGURATION ON  
IGNITION DELAY IN A 50-POUND-THRUST ROCKET

By Dezso J. Ladanyi

SUMMARY

Ignition delays of a diallylaniline-triethylamine mixture (57 percent diallylaniline and 43 percent triethylamine by weight) and triethyl trithiophosphite with red fuming nitric acid were measured at simulated altitude conditions with a rocket engine of approximately 50 pounds thrust.

Ignition delay usually increased with an increase in combustor diameter and length and exhaust-nozzle diameter. A decrease in propellant temperature also increased the delay, but initial ambient pressure was unimportant except for the largest nozzle diameter.

The data are best fitted by an empirical equation relating ignition delay to combustor dimensions, nozzle area, and propellant temperature. A possible theoretical basis for the correlation is discussed, as well as extension of the results to other systems.

INTRODUCTION

The importance of ignition delay as a criterion in the selection of a self-igniting liquid rocket-propellant combination is well recognized. Knowledge of ignition delay is also important in designing starting systems for rocket engines. There is no standard method for measuring this parameter, and data obtained by different methods for the same propellants at the same initial conditions often vary.

Some attempts have been made to standardize ignition-delay apparatus (e.g., refs. 1 and 2). Restrictions were usually placed on the chemical uniformity of the propellants and the temperatures at which the experiments were conducted. Sometimes oxidant-fuel ratios were also specified. Since considerable freedom was allowed in the manner of bringing the propellants together and in the size and shape of the reaction vessel, discrepancies in the results could be expected and did occur.

Only a few studies have been made on the influence of factors other than initial propellant temperature and ambient pressure on ignition delay (e.g., refs. 3 to 5). Moderate changes in variables such as propellant-injection pressure and oxidant-fuel ratio had relatively little effect on ignition delay. To determine the importance in ignition-delay measurements of combustion-chamber configuration, the NACA Lewis laboratory conducted a series of experiments with a small-scale rocket engine. The effects of chamber length, chamber diameter, and exhaust-nozzle size were determined at temperatures from  $120^{\circ}$  to  $-90^{\circ}$  F and at initial pressure altitudes of zero and 90,000 feet.

The results of this study, which also included a few related experiments with changes in injection method, combustor surface area, and injection pressure, are presented herein. An empirical correlation among ignition delay, combustor dimensions, nozzle area, and initial propellant temperature is presented. Possible theoretical significance of the correlation is discussed, as well as extension of the results to other systems.

#### APPARATUS

The ignition-delay apparatus used in this investigation is shown in figure 1. It consisted of a 50-pound-thrust rocket engine plus other components described in references 6 and 7. The only modification was a hydraulic system for rapidly assembling the rocket engine.

As shown in the insert of figure 1(a), the rocket-engine assembly consists of an injector head, injector orifices, a transparent cylindrical combustion chamber, a plate with a convergent exhaust nozzle, and propellant tanks.

Internally, the engine is similar to the one in reference 6. The  $90^{\circ}$  included angle of the propellant streams, the center location of the combustion-chamber pressure tap in the injector head, and the 0.041-inch fuel-injector-hole diameter are all unchanged. The 0.0675-inch oxidant-injector-hole diameter is the same as the one in reference 7, and 0.2-, 0.4-, and 0.8-inch-throat-diameter exhaust nozzles were also employed.

In addition to the 4-inch-long, 2-inch-inside-diameter combustion chamber used in all previous studies with this apparatus, 19 other sizes were employed in this investigation. They ranged from 1 inch long with a 1-inch inside diameter to 8 inches long with a 4-inch inside diameter, and are listed in the first two columns of table I. Two engine assemblies representing the extreme combustion-chamber sizes are shown in figure 2. Hereinafter, the size of a chamber is designated by two numbers representing its nominal length and diameter, respectively. For example, a  $6 \times 2$  chamber is 6 inches long and has a 2-inch inside diameter.

To strengthen some of the larger diameter chambers, 1/2-inch-wide steel bands were clamped around them approximately 1/2 inch apart. One to six bands were used, depending on chamber length.

To increase the surface area without changing the volume, three modifications of the standard 4×2 cylinders were used (fig. 3). In one, the inside wall was sand blasted. The actual increase in area could not be measured readily; however, if hemispherical depressions are assumed, the increase in the plastic-wall area is almost double. In another one, 28 plastic fins were attached to the inside wall, the diameter of which had been increased to  $2\frac{1}{8}$  inches so that the volume would remain constant. The fins were 3/16 inch high and 1/8 inch wide. The new inner-surface area was slightly more than  $2\frac{1}{2}$  times that of the unmodified chamber. The third cylinder was cut with a 45°, 24-turn-per-inch thread, which increased the area approximately one-half.

As shown in figure 4, the injector head and nozzle plate of references 6 and 7 were modified with additional grooves to accept the 3- and 4-inch-diameter chambers. To permit the use of 1-inch-diameter cylinders, the removable, injector-head inserts were replaced by orifices located integrally in the head.

In some auxiliary experiments, a two-on-one injector was used. In this modification, shown in figure 5, two oxidant streams at an included angle of 90° impinge on a centrally located fuel stream. This method of injection yields an axially directed propellant spray rather than the sidewise-directed resultant obtained from the standard one-on-one system. Oxidant-fuel weight ratios, propellant flow rates, point of jet impingement, and length of stream travel before impingement were all equivalent in the two injection methods. The only changes were a relocation of the combustion-chamber pressure tap, as indicated in figure 5, and a smaller oxidant jet diameter.

In order to check some of the conclusions, runs were made with 5×2 chambers and 0.3-inch-diameter exhaust nozzles, neither of which were used in the investigation proper.

#### PROCEDURE

The operating procedure is described in reference 6. An electrical program timer controlled the operation of the apparatus. When a fast-acting solenoid valve was opened, pressurized helium ruptured sealing disks at the upper ends of the propellant tanks. The pressure was then transmitted to the propellants, which burst the lower sealing disks and entered the combustion chamber where the ensuing events were recorded by a high-speed camera. Usually, the propellant-injection pressure was

approximately 450 pounds per square inch gage. In two runs, which were the only exceptions, the pressure was approximately 600 pounds per square inch gage. Runs were considered satisfactory for use as data when no significant operational difficulties were observed. Ignition delay  $\tau$  is defined as the time interval between contact of propellants and appearance of a persistent flame.

### PROPELLANTS

Two fuels were used in this investigation. Most of the runs were made with a fuel blend containing 57 percent diallylaniline and 43 percent triethylamine by weight. Unless otherwise specified, all discussions pertain to this fuel. The other fuel was triethyl trithiophosphite. Physical properties of these fuels have been reported previously (refs. 6 and 7).

The oxidant used with each of the fuels was red fuming nitric acid containing 3 to 4 percent water and 19 to 20 percent nitrogen dioxide by weight.

### RESULTS

Of the total 193 satisfactory runs, the majority (136 runs) were made with the diallylaniline-triethylamine mixture and red fuming nitric acid at sea-level pressure and at temperatures from 120° to -90° F. A summary of the data is presented in tables II to VI.

Sixteen other runs were made with the same propellant combination in the same temperature range, but at a pressure altitude of approximately 90,000 feet (table VII). Most of these runs were conducted at the two temperature limits of 120° and -90° F and with the extreme chamber sizes.

Some miscellaneous experiments with diallylaniline-triethylamine mixture and red fuming nitric acid were performed. Twenty-five runs were made with extended-surface plastic chambers (table VIII); two, with propellant-injection pressures other than the standard 450 pounds per square inch gage (table III); seven, with two-on-one injectors (tables III and VI); and seven, with new combustion-chamber configurations to check some conclusions obtained from the analysis of the data (table IX).

Seven runs were made with another propellant combination - triethyl trithiophosphite and red fuming nitric acid (table X).

### Effect of Chamber Length

With all other parameters constant, ignition delay generally increased with an increase in the length of the chamber. An illustration of the general relation between ignition delay  $\tau$  and chamber length  $L$  for various chamber diameters and nozzle sizes is shown in figure 6 for 120° F and sea-level pressure.

### Effect of Chamber Diameter

Without exception, ignition delay increased with an increase in chamber diameter when all other parameters were held constant. This effect of combustion-chamber diameter  $D$  on delay is illustrated in figure 7 for 120° F and sea-level pressure. With respect to ignition delay, the relatively larger effect of diameter over length is shown by a comparison of the numerical values of the slopes of figures 6 and 7. Depending on the chamber and exhaust-nozzle diameters, the rate of change of ignition delay with length varies from 0.7 to 5.3 milliseconds per inch. A comparable range for the diameter is 5.0 to 13.3 milliseconds per inch.

### Effect of Exhaust-Nozzle Diameter

Ignition delay generally increased when the only change was an increase in the exhaust-nozzle diameter  $D_n$ . Some examples showing this effect are presented in figure 8.

### Effect of Temperature

For any particular chamber configuration, nozzle size, propellant combination, and initial ambient pressure, the ignition delay increased with a decrease in propellant temperature. This trend is consistent with all previous results obtained with the small-scale rocket-engine apparatus.

The ignition-delay temperature relation for the diallylaniline-triethylamine mixture was determined in smaller increments for a 4×2 chamber and a 0.4-inch-diameter exhaust nozzle than for any of the other combinations. The results are summarized in table II and plotted in figure 9. For comparison, a similar relation of the same fuel with a slightly different acid (ref. 6) is also plotted on figure 9. This graph shows a rapid rise of delay below -60° F. Similar results were obtained with other chamber and nozzle sizes. Since this sudden rise occurs in the same temperature range as a similar sharp rise in the viscosity of the fuel, some correlation between viscosity and ignition delay is suggested. Such a possible correlation has already been discussed in references 2, 4, and 8.

### Effect of Initial Ambient Pressure

Previous studies conducted with the 50-pound-thrust rocket engine have shown that variations of initial ambient pressure altitude from sea level to about 90,000 feet produce no significant changes in ignition delay. Explanations for these observations are presented in references 6 and 7. In this investigation, similar results were obtained with exhaust nozzles of 0.2- and 0.4-inch diameter. With an 0.8-inch-exhaust-nozzle diameter, however, the chamber was effectively no longer a totally enclosed cylinder, and the increase in ignition delay at 90,000 feet over that at sea level was appreciable at high temperatures and even greater at low temperatures. These differences are shown in table XI.

### Effect of Various Chamber-Wall Surfaces

Some experiments were conducted with 4×2 chambers in which the smooth inner wall was modified as described previously. All these runs were made at 120° F with a nozzle diameter of 0.4 inch. There were thirteen runs made with the screw-threaded chambers; one with a sand-blasted chamber; and eleven with finned chambers. The data are summarized in table VIII. For comparison, runs with smooth-walled chambers are also included. A condensed form of the results along with other pertinent information is presented in table XII.

The results show that surface profile has practically no effect on ignition delay. There are only small differences between the average delays obtained with the screw-threaded, sand-blasted, and plain chambers. The average delay for the finned chambers is only slightly longer than that for plain chambers in spite of the large increase in surface area.

### Effect of Propellant-Injection Pressure

In references 3 and 6, it is reported that ignition delay decreased with an increase in propellant-injection pressure and that the rate of decrease diminished until there was no further significant change in delay with injection pressure. In this study, two check runs at approximately 600 pounds per square inch gage (table III) yielded no significant changes in ignition delay, indicating that the plateau had been attained at the standard injection pressure of 450 pounds per square inch gage.

### Effect of Propellant-Injection Method

Most of the runs reported herein were conducted with the one-on-one injection system in which the resultant spray of the impinging jets was at an angle to the chamber axis. To determine whether the results could

be extended to other injection systems, several runs (tables III and VI) were made with the two-on-one injector mentioned in a previous section. This injector produced a resultant stream which was directed axially towards the nozzle exit. Ignition delays obtained with the two injector types were approximately the same (table XIII), and it appears probable that the close relation is similar at other conditions as well.

### Effect of Different Fuels

Ignition delays measured in the small-scale rocket engine for the diallylaniline-triethylamine mixture and triethyl trithiophosphite with red fuming nitric acid over wide temperature and pressure ranges have been reported previously (refs. 6 and 7). In those determinations, the standard 4×2 chamber with a 0.4-inch nozzle was used. In the present study the triethyl trithiophosphite - red fuming nitric acid combination was re-examined with the standard 0.4-inch nozzle at extreme chamber sizes and temperatures. A summary of the data is presented in table XIV. For comparison, diallylaniline-triethylamine runs at the same conditions are also tabulated. In every case, the more reactive triethyl trithiophosphite yielded shorter delays than the diallylaniline mixture. Figure 10 illustrates the magnitude of the differences.

### DISCUSSION

Ignition lag should depend largely on the concentration of active particles which lead to ignition, and the quenching of these particles at the reactor walls or complete removal of the particles from the reactor. Wall quenching is discussed in reference 9. For a closed reactor with dimensions that are large compared with the mean free path of the reactant molecules and with a fixed charge, ignition lag should vary mostly with concentration, that is, with reactor volume. For an open tube with subcritical flow, on the other hand, concentration will be determined by the exit pressure, and ignition lag should vary with ambient pressure. The two other factors important in this case are flow turbulence that should increase the importance of wall quenching by promoting diffusion, and removal of material at the end of the tube that should also effectively retard the reactions. The removal of material should decrease in importance as tube length is increased. In the open tube, then, ignition lag should depend on chamber length and diameter as well as ambient pressure.

The combustor used for this study with its variable nozzle area lies between the two extremes just mentioned. On the basis of the above discussion, it is expected that ignition lag will vary with volume and to some extent with surface area. As nozzle area is increased, the effects of material removal and ambient pressure should increase in magnitude. In the following discussion the results are analyzed in terms of these views.

### Relation Between Ignition Delay and Combustor Dimensions

With other factors constant, ignition delay was plotted against independent parameters involving chamber length and diameter such as chamber volume, characteristic length, inner surface area, and surface-to-volume ratio. The best correlation (fig. 11) was obtained when ignition delay  $\tau$  was plotted against total inner-surface area  $A_t$ , which consisted of the sum of the areas of the injector face, exhaust-nozzle plate, and the cylindrical plastic wall. (Table I lists  $A_t$  for the different lengths and diameters.)

Since a change in inner-surface area was generally accompanied by a corresponding change in combustor volume, the combustor volume is implicitly included in the correlation. The relative importance of volume and surface are not apparent in figure 11; however, data from auxiliary experiments with constant volume-variable surface combustors, which will be discussed later, show that volume is the predominant factor in this correlation.

To obtain a single correlation of ignition delay with inner-surface area and temperature, the slopes of the lines in figure 11 were plotted against temperature in figure 12. The slopes were chosen to fit the data for the smallest nozzle diameter and are the same for all three nozzles at each temperature. The resultant equation is

$$\log \tau = \log A_t - 0.001608 T - 0.211 \quad (1)$$

where  $T$  is temperature in degrees Fahrenheit,  $A_t$  is inner-surface area in square inches, and  $\tau$  is ignition delay in milliseconds. Although it does not account for material removal through the nozzle, this equation illustrates the relative importance of geometry and temperature on the delay. It might also be written in the Arrhenius-type form

$$\tau = k A_t e^{aT+b} \quad (2)$$

where  $a$  and  $b$  are constants which depend on the propellants, and  $k$  is a dimensional constant.

### Effect of Nozzle Area on Ignition Delay

The correlation of ignition delay with surface area deteriorates as nozzle diameter is increased, especially at low temperatures. It may be assumed that the deviations from equation (1) are mainly due to loss of reacting materials through the nozzle. This effect should vary with combustor length and diameter and initial temperature and pressure, as well

as actual nozzle area, and may be treated as an addition to inner-surface area. From the deviations, the following empirical equation was derived (shown in the appendix) for the effective nozzle area  $A_n^*$  in terms of the actual nozzle area  $A_n$ , the chamber length  $L$ , the chamber diameter  $D$ , and the propellant temperature  $T$ :

$$A_n^* = A_n [(0.1307 L - 1.051) T - 28.83 L + 253.15] + (0.00143 T - 0.271)(D - 1)$$

where  $A_n^*$  and  $A_n$  are in square inches,  $L$  and  $D$  are in inches, and  $T$  is in degrees Fahrenheit. The data were insufficient for establishing the effect of pressure.

The term  $A_t$  in equation (1) may then be replaced by an effective surface area  $A_t^*$ , which is the sum of  $A_t$  and  $A_n^*$ , so that

$$\log \tau = \log(A_t + A_n^*) - 0.001608 T - 0.211 \quad (3)$$

or

$$\log \tau = \log A_t^* - 0.001608 T - 0.211 \quad (4)$$

Values of  $A_n^*$  and  $A_t^*$  are listed in table I.

A plot of ignition delay against effective surface area is shown in figure 13 and indicates the improvement in the correlation over that of figure 11. Figure 13(e) presents a combined plot of ignition delay against effective surface area for several temperatures. For convenience, equation (4) which represents the average delay is plotted in figure 14 together with the data points from figure 13. Selected points at comparable effective surface areas are shown in table XV to illustrate the precision of the correlation.

#### Experimental Check of Nozzle-Area Correlation

To check the validity of the effective nozzle-area correlation, seven runs were made at 40° F with a 5×2 combustion chamber and a 0.3-inch-diameter exhaust nozzle. These particular values of the independent parameters had not been used in the original correlation. The results are summarized in table IX. The predicted ignition delay as calculated from equation (4) is 23.8 milliseconds. The average of the experimental ignition delays is 25.0 milliseconds. It appears, therefore, that the correlation of ignition delay with effective surface area is valid for interpolated values of the independent variables.

### Auxiliary Experiments

Low-pressure effects. - As discussed earlier, a change in initial ambient-pressure altitude from sea level to 90,000 feet does not affect ignition delay significantly as long as the exhaust-nozzle diameter is 0.4 inch or less. With an 0.8-inch nozzle, however, ignition delays at 90,000 feet are much larger than at sea-level, especially at low temperatures (-90° F). On the basis of previous discussion, this effect may be attributed to an increase in the rate of the reactant loss through the exhaust nozzle. Thus, the larger the nozzle diameter, the closer the behavior of this reactor approaches that of an open tube. At the low temperatures the situation is further aggravated by slower initial reaction rates and poorer injector mixing caused by increased viscosity. The effective nozzle area should also be a function of pressure and the correlating equation should include this factor. It was omitted, however, since the number of runs made at the low pressure was insufficient for a quantitative correlation.

Area-volume experiments. - Although the best direct correlation was between ignition delay and total surface area, the influence of chamber volume in the correlation is implicit since, for every area change, there was usually a change in volume.

To determine separately the influence of chamber volume and surface on ignition delay, experiments were conducted with the extended-surface combustors described previously. It is apparent from the data (table XII) that reactor surface area is less important than volume in determining ignition lag. The relative importance of wall quenching and, hence, surface area should increase as volume decreases or as reactor diameter decreases since this would cause a decrease in the diffusion distance to the wall.

Propellant-combination variations. - The more reactive triethyl trithiophosphite yielded a shorter ignition delay than the diallylaniline-triethylamine mixture for every comparable set of conditions. For this reason, a plot of ignition delay against the effective inner surface area of the chamber for both fuels should yield two lines with the thiophosphite data having the smaller slope. Such a plot is shown in figure 15 where the effective nozzle area relation was assumed to be the same for both fuels. The main inference drawn from this figure is that, regardless of the propellant combination, almost any required ignition delay may be approximated if the proper chamber dimensions are chosen. This information is useful if the selection of a certain propellant combination is mandatory and if the ignition delay is the most important consideration; otherwise, the effects of chamber-size manipulation on other factors in rocket-engine design must be evaluated.

## CONCLUDING REMARKS

The results of this study illustrate how sensitive ignition lag is to changes in reactor geometry. Using the correlation, however, makes possible extending the results in order to predict the effects of design changes in similar combustor configurations.

Extension of equation (4) to other fuels becomes relatively simple if the assumption is made that effective nozzle area is not a function of the fuel used. For most fuel-acid systems where the weight ratio of fuel to acid is low this is not an unreasonable assumption. As was the case in this study, the lines of ignition lag against effective surface area for different fuels would differ only in slope. For a given temperature, the slope could be determined by one reliable value of ignition delay at a known value of effective surface area. Equation (4) could then be used for the new fuel with a correction for the difference in slope.

## SUMMARY OF RESULTS

Ignition-delay determinations of two fuels with a low-freezing-point red fuming nitric acid were made at simulated altitude conditions with a rocket engine of nominally 50 pounds thrust.

The results of this study may be summarized as follows:

1. For the fuel mixture of 57 percent diallylaniline and 43 percent triethylamine by weight, ignition delay increased when each of the following parameters was independently varied:

- (a) Chamber length increased (1 to 8 in.)
- (b) Chamber diameter increased (1 to 4 in.)
- (c) Nozzle diameter increased (0.2 to 0.8 in.)
- (d) Propellant temperature decreased ( $120^{\circ}$  to  $-90^{\circ}$  F)
- (e) Pressure decreased (30 and 0.5 in. Hg) with 0.8-inch-diameter nozzle only; no change with 0.2- and 0.4-inch-diameter nozzles
- (f) Surface area increased

2. For the same fuel, ignition delay was unaffected by small changes in injection pressure and by an injector change from a one-on-one to a two-on-one impinging jet system.

3. Observations (a) to (d) were also noted for the second fuel, triethyl trithiophosphite. In every comparable instance, this fuel gave shorter ignition delays than the diallylaniline-triethylamine blend.

4. The data are correlated in terms of combustor dimensions, initial propellant temperature, and effective nozzle area. The effective nozzle area is a function of combustor length and diameter and initial propellant temperature.

Lewis Flight Propulsion Laboratory  
National Advisory Committee for Aeronautics  
Cleveland, Ohio, June 22, 1956

## APPENDIX - DERIVATION OF EFFECTIVE NOZZLE AREA

Several simplifying assumptions were made and are presented in the course of the derivation. One major assumption was that the deviations from equation (1) were due to the influence of flow through the nozzle. Thus an effective nozzle area added to the surface area would correct the deviations. The effective nozzle area was further assumed to be a function of actual nozzle area, combustor length, propellant temperature, ambient pressure, and possibly combustor diameter.

### Contribution of Actual Nozzle Size

With temperature, chamber length, and chamber diameter held constant, a plot of effective nozzle area against actual nozzle area was best fitted by a complex curve represented by an equation of greater than first order. For simplification, a straight line with a positive slope was assumed to be sufficiently accurate provided that two conditions were fulfilled. These were that (1) the effective nozzle area could never be less than the actual nozzle area (2) that the two had to be zero simultaneously (shown in fig. 16). A general equation representing the curve has the form

$$A_n^* = kA_n \quad (5)$$

where  $k$  is a constant which applies only for a particular temperature, chamber diameter, and chamber length.

### Contribution of Chamber Length

The contribution of chamber length to the nozzle effect can be determined when the effective nozzle area is plotted against length, holding temperature, chamber diameter, and actual nozzle-area constant. The resultant curve should have the general shape of a hyperbola with asymptotes to both axes. This shape is obtained because, as the chamber length attains large values, the nozzle effect becomes insignificant. Conversely, as the length decreases and the intersection of the propellant jets approaches the nozzle hole, the effective nozzle area becomes infinitely large. In the range of chamber lengths used in this investigation, however, the curve is essentially a straight line, especially for the shorter chambers. For simplification, therefore, a negative-sloped linear relation was assumed as shown by the general expression

$$A_n^* = aL + b \quad (6)$$

where  $a$  and  $b$  are constants whose values depend on the magnitude of the other parameters.

Combining equations (5) and (6) yields an expression in which the effective nozzle area is a function of both actual nozzle size and chamber length:

$$A_n^* = k' A_n (aL + b) \quad (7)$$

where  $k'$  is a constant which applies for a particular temperature and chamber diameter. A series of curves obtained by equation (7) for  $120^\circ F$  and a 1-inch-diameter chamber is shown in figure 17.

#### Contribution of Propellant Temperature

When effective nozzle area is plotted against temperature for selected values of chamber diameter, chamber length, and nozzle diameter, hyperbolic-type curves should be obtained. These curves show that the nozzle effect rapidly becomes very small as the temperature is increased because of the rapid increase in reaction rate, and also they show a converse effect as the temperature is decreased because of slower reaction rates and poorer mixing efficiencies caused by rapidly increasing propellant viscosities. Again for simplification, a linear relation with a negative slope is assumed between effective nozzle area and temperature. The general equation showing this relation is

$$A_n^* = cT + d \quad (8)$$

where the constants  $c$  and  $d$  depend on the other parameters.

If equation (8) is combined with equation (7), an over-all expression for effective nozzle area is obtained which accounts for all the variables except chamber diameter. A general form is

$$A_n^* = A_n [(a'L + b') T + a''L + b''] \quad (9)$$

where  $a'$ ,  $b'$ ,  $a''$ , and  $b''$  are constants whose values depend only on the chamber diameter. Examples of curves derived from equation (9) are shown by figure 18.

#### Contribution of Chamber Diameter

The contribution of chamber diameter to the nozzle effect is quite small when compared with the contributions of the other parameters. This is observed when effective nozzle area is plotted against diameter for various values of nozzle area, chamber length, and propellant temperature.

As discussed previously, the nozzle effect decreases with an increase in chamber diameter. For simplification, a linear relation between effective nozzle area and diameter was assumed and may be represented generally as

$$A_n^* = eD + f \quad (10)$$

where the constants  $e$  and  $f$  are assumed to depend solely on temperature in a linear manner. This assumption was made so that the final expression for  $A_n^*$  would not be greater than third order. Since the magnitude of the contribution of diameter on the nozzle effect is small, none of these assumptions can lead to significant errors.

A combination of equations (9) and (10) yields a general expression for the effective nozzle area in terms of all the quantitatively investigated variables. This final equation is

$$A_n^* = A_n [(a'L + b') T + a''L + b''] + (a''' T + b''')(D-1) \quad (11)$$

The same equation, with numerical constants obtained from curves drawn according to the foregoing assumptions, is

$$A_n^* = A_n [(0.1307 L - 1.051) T - 28.83 L + 253.65] + (0.00143 T - 0.271)(D-1) \quad (12)$$

and was used to supply values of effective nozzle area for equation (4).

#### REFERENCES

1. Strier, M.: The Correlation and Evaluation of the Results of the Standard Ignition Delay Test Program. Rep. RMI-499-S1, Reaction Motors, Inc., Apr. 22, 1953. (Contract NOas 52-595-C, RMI Proj. 499.)
2. Burgess, G. S., and Kuchta, J. N.: Performance Characteristics of Hydrocarbon-Based Rocket Fuels. Prog. Rep. No. 6, Bur. Mines, Sept. 30, 1953.
3. Anon.: Combined Bimonthly Summary No. 8 - Aug. 20-Oct. 20, 1948. Jet Prop. Lab., C.I.T., Nov. 15, 1948.
4. Adelman, Barnet R.: A Study of Ignition-Lag Characteristics of Some Liquid Rocket Fuels with Red Fuming Nitric Acid, Including Additives to the Oxidizer. Prog. Rep. No. 20-138, Jet Prop. Lab., C.I.T., Apr. 18, 1951. (Ord. Contract DA-04-495-ORD-18.)

5. Anon.: Combined Bimonthly Summary No. 10, Dec. 20, 1948 - Feb. 20, 1949. Jet Prop. Lab., C.I.T., March 15, 1949.
6. Ladanyi, Dezso J.: Ignition Delay Experiments with Small-Scale Rocket Engine at Simulated Altitude Conditions Using Various Fuels with Nitric Acid Oxidants. NACA RM E51J01, 1952.
7. Ladanyi, Dezso J., and Hennings, Glen: Organophosphorus Compounds in Rocket-Engine Applications. NACA RM E54A26, 1954.
8. Ladanyi, Dezso J.: Orthotoluidine and Triethylamine in Rocket Engine Applications. NACA RM E52K19, 1953.
9. Belles, Frank E., and Berlad, A. L.: Chain Breaking and Branching in the Active-Particle Diffusion Concept of Quenching. NACA TN 3409, 1955.

TABLE I. - DESCRIPTIVE CHARACTERISTICS OF COMBUSTION CHAMBERS HAVING VARIOUS LENGTHS, DIAMETERS, AND EXHAUST-NOZZLE SIZES  
 [Effective nozzle area,  $A_n^*$ , sq in.; total effective surface area,  $A_t^*$ , sq in.]

Length, L, in.	Diameter, D, in.	Exhaust-nozzle diameter, $D_n$ , in.			Volume, V, cu in.	Temperature, °F																
		$a_{0.2}$				120								68		0		-90				
		$a_{0.4}$				Exhaust-nozzle diameter, $D_n$ , in.								$a_{0.2}$		$a_{0.4}$		$a_{0.8}$		$a_{0.2}$		
		$a_{0.8}$				$A_n^*$	$A_t^*$	$A_n^*$	$A_t^*$	$A_n^*$	$A_t^*$	$A_n^*$	$A_t^*$	$A_n^*$	$A_t^*$	$A_n^*$	$A_t^*$	$A_n^*$	$A_t^*$	$A_n^*$	$A_t^*$	
1	1	3.8	3.7	3.3	0.8	3.6	7.4	14.4	18.1	57.5	60.8	5.1	8.9	28.3	32.0	9.7	13.5	38.7	42.4	154.7	158.0	
2	1	6.9	6.8	6.5	1.6	3.2	10.1	12.7	19.5	50.9	57.4	4.5	11.4	24.6	31.4	8.4	15.3	33.6	40.4	134.3	140.8	
4	1	13.2	13.1	12.8	3.1	2.4	15.6	9.4	22.5	37.7	50.5	3.2	16.4	17.4	30.5	5.8	19.0	23.4	36.5	93.4	106.2	
6	1	19.5	19.4	19.0	4.7	1.5	21.0	6.1	25.5	24.5	43.5	2.0	21.5	10.1	29.5	3.3	22.8	13.2	32.6	52.6	74.6	
8	1	25.8	25.7	25.3	6.3	.7	26.5	2.8	28.5	11.2	36.5	.7	26.5	2.9	28.6	.7	26.5	3.0	28.7	11.8	37.1	
1	2	11.8	11.7	11.3	3.1	3.5	15.3	14.3	26.0	57.4	68.7	4.9	16.7	28.0	39.7	9.3	21.1	38.3	50.0	154.3	165.6	
2	2	18.0	17.9	17.6	6.3	3.1	21.1	12.6	30.5	50.8	68.4	4.3	22.3	24.4	42.3	8.0	26.0	33.2	51.1	133.9	151.5	
4	2	30.6	30.5	30.1	12.6	2.3	32.9	9.3	39.8	37.6	67.7	3.1	33.7	17.1	47.6	5.4	36.0	23.0	53.5	93.0	123.1	
6	2	43.2	43.1	42.7	18.8	1.4	44.6	6.0	49.1	24.4	67.1	1.8	45.0	9.9	53.0	2.9	46.1	12.8	55.9	52.2	94.9	
8	2	55.7	55.6	55.2	25.1	.6	56.3	2.7	58.3	11.1	66.3	.5	56.2	2.6	58.2	.3	56.0	2.6	58.2	11.4	66.6	
1	3	21.9	21.8	21.4	7.1	3.4	25.3	14.2	36.0	57.3	78.7	4.8	26.7	27.7	49.5	8.9	30.8	37.9	59.7	153.9	175.3	
2	3	31.3	31.2	30.8	14.1	3.0	34.3	12.5	43.7	50.7	81.5	4.1	35.4	24.1	55.3	7.6	38.9	33.8	65.0	133.5	164.3	
4	3	50.1	50.0	49.7	28.3	2.2	52.3	9.2	59.2	37.5	87.2	2.9	53.0	16.9	66.9	5.0	55.1	22.6	72.6	92.6	142.3	
6	3	69.0	68.9	68.5	42.4	1.3	70.3	5.9	74.8	24.3	92.8	1.6	70.6	9.6	78.5	2.5	71.5	12.4	81.3	51.8	120.3	
8	3	87.8	87.7	87.3	56.5	.5	88.3	2.6	90.3	11.0	98.3	.4	88.2	2.4	90.1	.0	87.8	2.2	89.9	11.0	98.3	
1	4	35.1	35.0	34.7	12.6	3.3	38.4	14.1	49.1	57.2	91.9	4.6	39.7	27.4	62.4	8.5	43.6	37.5	72.5	153.5	188.2	
2	4	47.7	47.6	47.2	25.1	2.9	50.6	12.4	60.0	50.6	97.8	4.0	51.7	23.8	71.4	7.2	54.9	33.4	81.0	133.1	180.3	
4	4	72.8	72.7	72.3	50.3	2.1	74.9	9.1	81.8	37.4	109.7	2.7	75.5	16.6	89.3	4.6	77.4	22.2	94.9	92.2	164.5	
6	4	98.0	97.9	97.5	75.4	1.2	99.2	5.8	103.7	24.2	121.7	1.5	99.5	9.3	107.2	2.1	100.1	12.0	109.9	51.4	148.9	
8	4	123.0	122.9	122.6	100.5	.4	123.4	2.5	125.4	10.9	133.5	.2	123.2	2.1	125.0	.0	123.0	1.8	124.7	10.6	133.2	

TABLE II. - SUMMARY OF IGNITION DATA AT SEVERAL TEMPERATURES AND SEA-LEVEL PRESSURE FOR A DIALLYLANILINE-  
TRIETHYLAMINE MIXTURE AND RED FUMING NITRIC ACID

[4-In.-long, 2-in.-inside-diameter combustion chamber; 0.4-in.-diameter exhaust nozzle.]

Run	Average propellant temperature, °F	Maximum combustion-chamber pressure, lb/sq in. gage	Time to attain maximum combustion-chamber pressure, sec	Temperature, °F			Propellant-injection pressure, lb/sq in. gage	Lead propellant into combustion chamber	Time between jet entries into combustion chamber, millsec	Time between ignition and normal combustion picture, millsec	Ignition delay, millsec
				Oxidant	Fuel	Ambient air					
656	120	a254	b1.5	120	120	79	447	Fuel	20.0	0.2	14.8
655	120	a251	b1.6	120	120	78	447	Fuel	22.0	.4	15.2
654	120	a224	b1.5	119	120	76	447	Fuel	17.9	.3	15.4
425	99	310	.6	99	99	67	448	Oxidant	12.0	.8	12.9
365	79	a268	b.7	79	79	70	443	Fuel	1.1	.9	16.6
366	60	293	.9	60	60	73	443	Fuel	23.1	.7	14.1
367	40	a185	b.4	41	39	73	444	Oxidant	17.1	.4	20.6
426	20	308	.5	20	21	65	445	Fuel	1.1	.4	25.7
457	1	304	.4	1	2	66	448	Oxidant	.3	1.0	24.1
427	0	308	.4	1	0	56	447	Oxidant	25.8	.8	33.5
428	-20	308	.4	-20	-19	58	449	Oxidant	11.1	.6	30.2
374	-59	273	1.5	-59	-58	51	446	Oxidant	46.3	.9	49.7
430	-69	305	.6	-69	-69	62	452	Oxidant	28.9	1.1	51.1
577	-83	253	.5	-83	-83	63	445	Oxidant	2.6	1.8	51.7
382	-92	317	.9	-92	-92	66	456	Oxidant	(c)	.6	58.9

<sup>a</sup>Peak pressure; maximum pressure possible was probably not attained.

<sup>b</sup>Time to attain peak combustion-chamber pressure.

<sup>c</sup>No proper record.

TABLE III. - SUMMARY OF IGNITION DATA AT 120° F AND SEA-LEVEL PRESSURE FOR A DIALLYLANILINE-  
TRIETHYLAMINE MIXTURE AND RED FUMING NITRIC ACID

(a) 0.2-Inch-diameter exhaust nozzle

Run	Average propellant temperature, °F	Maximum combustion-chamber pressure, lb/sq in. gage	Time to attain maximum combustion-chamber pressure, sec	Temperature, °F			Propellant-injection pressure, lb/sq in. gage	Combustion-chamber length, in.	Combustion-chamber diameter, in.	Lead propellant into combustion chamber	Time between jet entries into combustion chamber, millisecond	Time between ignition and full combustion picture, millisecond	Ignition delay, millisecond
				Oxidant	Fuel	Ambient air							
625	120	320	1.1	120	120	78	448	1	1	Fuel	20.5	0.7	2.5
626	120	335	1.5	120	120	80	449	1	1	Fuel	7.4	.2	3.1
520	120	402	.5	120	120	(a)	448	2	2	Fuel	22.7	.6	8.0
580	121	(b)	(b)	122	121	81	448	2	3	Fuel	10.6	.3	16.0
524	120	c 250	d .3	119	121	(a)	448	2	4	Fuel	6.5	2.9	18.4
549	120	250	.4	119	121	(a)	446	4	2	Fuel	8.5	.5	13.7
578	120	393	.5	120	120	81	445	4	3	Oxidant	15.7	.8	23.4
606	119	170	.7	120	119	80	443	4	4	Fuel	15.9	.5	26.7
548	119	203	.3	119	118	76	447	6	2	Fuel	10.3	1.1	17.2
564	120	384	.4	120	121	79	452	6	3	Fuel	7.4	1.1	25.5
563	120	355	.9	(a)	120	78	443	6	4	Fuel	18.8	1.0	38.0
697	120	410	.3	120	120	79	445	8	2	Fuel	38.3	1.2	14.6
569	123	290	.6	123	123	(a)	447	8	2	Fuel	6.7	1.5	31.1
515	119	405	.6	119	119	77	443	8	3	Fuel	2.2	2.6	34.7
514	119	c 380	d .4	119	119	76	448	8	4	Fuel	6.1	2.6	39.3
581	120	c 310	d .5	120	120	79	447	8	4	Fuel	6.1	2.4	61.9

<sup>a</sup>No record obtained.<sup>b</sup>Explosion destroyed chamber 2 millisecond after ignition.<sup>c</sup>Peak pressure; maximum pressure possible was probably not attained.<sup>d</sup>Time to attain peak combustion-chamber pressure.

TABLE III. - Continued. SUMMARY OF IGNITION DATA AT 120° F AND SEA-LEVEL PRESSURE FOR A DIALLYLANILINE-  
TRIETHYLAMINE MIXTURE AND RED FUMING NITRIC ACID

## (b) 0.4-Inch-diameter exhaust nozzle

Run	Average propellant temperature, °F	Maximum combustion-chamber pressure, lb/sq in. gage	Time to attain maximum combustion-chamber pressure, sec	Temperature, °F			Propellant-injection pressure, lb/sq in. gage	Combustion-chamber length, in.	Combustion-chamber diameter, in.	Lead propellant into combustion chamber	Time between jet entries into combustion chamber, millisecond	Time between ignition and full combustion picture, millisecond	Ignition delay, millisecond
				Oxidant	Fuel	Ambient air							
600	118	80	0.6	115	120	77	447	1	1	Fuel	15.5	0.2	4.8
624	120	293	.8	119	121	82	587	1	1	Fuel	7.4	.2	5.2
602	120	73	.5	120	120	76	(a)	1	1	Fuel	14.4	.3	5.4
658	120	b228	c1.3	119	121	75	448	1	1	Fuel	3.6	.3	5.5
663	120	b170	c1.4	120	120	76	447	1	1	Fuel	18.2	.5	5.8
d659	120	b184	c1.4	120	120	79	448	1	1	Fuel	2.5	.3	6.3
622	120	200	1.2	120	121	78	452	1	1	Fuel	2.8	.3	6.4
623	120	b280	c.7	120	121	77	588	1	1	Fuel	2.4	<.2	7.1
662	120	b177	c1.4	120	120	80	449	1	1	Fuel	19.5	.2	7.2
641	120	215	1.5	120	120	72	451	1	1	Fuel	26.3	.2	7.5
661	120	b167	c1.1	120	120	76	449	1	1	Oxidant	.4	.4	7.5
657	120	b208	c1.3	120	120	71	450	1	1	Fuel	1.7	.2	9.0
660	120	b221	c1.4	120	120	77	449	1	1	Oxidant	2.8	.5	9.2
590	120	183	.9	119	121	82	445	1	1	Fuel	1.5	.3	12.0
717	120	276	.8	121	119	83	448	1	2	Fuel	32.3	.4	8.5
591	119	156	.5	119	120	79	444	1	2	Fuel	2.2	.5	13.5
700	120	b295	c.5	121	119	95	448	1	3	Fuel	2.9	.4	12.9
589	121	193	.8	121	122	75	(a)	1	3	Oxidant	1.1	.5	16.8
588	122	(e)	(e)	121	122	80	447	1	4	Fuel	7.7	.3	19.0
592	119	193	.8	119	119	78	447	2	1	Fuel	17.0	.2	5.8
642	120	260	.8	120	120	74	446	2	2	Fuel	22.6	.2	9.5
357	120	285	.7	(a)	120	89	440	2	2	(f)	Q.2	.6	12.9
d614	119	267	.7	119	120	77	446	2	2	Fuel	9.4	.5	13.1
485	121	300	.6	121	121	80	446	2	3	Fuel	22.7	.4	17.3
466	119	310	.7	119	119	76	447	2	4	Fuel	27.9	.7	25.9
584	120	260	.6	120	121	88	445	4	1	Fuel	10.4	.3	8.0
656	120	b254	c1.5	120	120	79	447	4	2	Fuel	20.0	.2	14.8
655	120	b251	c1.6	120	120	78	447	4	2	Fuel	22.0	.4	15.2
654	120	b224	c1.5	119	120	76	447	4	2	Fuel	17.9	.3	15.4
379	119	340	.5	120	119	77	450	4	3	Oxidant	34.1	1.9	20.6
377	119	333	.6	119	119	83	444	4	3	Fuel	8.4	.4	22.3
605	120	b110	c.6	120	120	78	447	4	3	Fuel	22.8	1.0	24.7
446	118	330	.5	118	118	48	451	4	4	Fuel	19.3	.6	31.0
586	120	288	.9	120	120	81	452	6	1	Fuel	1.9	.9	9.5
593	119	203	.6	118	120	72	446	6	2	Fuel	11.5	.3	16.9
353	119	b250	c.7	119	120	86	448	6	3	Fuel	8.4	.8	25.0
354	120	325	.4	120	120	82	449	6	4	Fuel	25.5	3.1	35.3
587	120	48	.8	120	121	85	438	8	1	Fuel	3.1	.8	9.3
445	119	(e)	(e)	119	119	69	448	8	2	Oxidant	37.6	.7	17.3
d634	119	289	.7	(a)	119	74	444	8	2	Fuel	11.9	1.0	25.0
463	121	(e)	(e)	121	120	77	449	8	2	Oxidant	3.0	.6	26.4
444	119	325	.3	119	119	67	446	8	3	Fuel	19.8	.7	34.6
594	122	b40	c.3	124	120	82	448	8	4	Fuel	2.7	.9	48.1
447	119	340	.5	119	119	72	446	8	4	Fuel	28.6	1.3	48.3
d612	120	285	.6	120	119	73	444	8	4	Fuel	7.0	2.4	48.4

<sup>a</sup>No record obtained.<sup>b</sup>Peak pressure; maximum pressure possible was probably not attained.<sup>c</sup>Time to attain peak combustion-chamber pressure.<sup>d</sup>Run made with two-on-one injector.<sup>e</sup>Explosion occurred < 2.5 millisecond after ignition.<sup>f</sup>Both propellants entered combustion chamber in same motion-picture frame.<sup>g</sup>Doubtful accuracy.

TABLE III. - Concluded. SUMMARY OF IGNITION DATA AT 120° F AND SEA-LEVEL PRESSURE FOR A DIALLYLANILINE-  
TRIETHYLAMINE MIXTURE AND RED FUMING NITRIC ACID

(c) 0.8-Inch-diameter exhaust nozzle

Run	Average propellant temperature, °F	Maximum combustion-chamber pressure, lb/sq in. gage	Time to attain maximum combustion-chamber pressure, sec	Temperature, °F			Propellant injection pressure, lb/sq in. gage	Combustion-chamber length, in.	Combustion-chamber diameter, in.	Lead propellant into combustion chamber	Time between jet entries into combustion chamber, millisec	Time between ignition and full combustion picture, millisec	Ignition delay, millisec
				Oxidant	Fuel	Ambient air							
573	120	44	0.5	120	120	(a)	447	2	2	Fuel	0.3	1.9	26.6
491	120	91	.6	120	120	76	446	2	3	Fuel	15.1	.5	27.6
492	120	95	.6	120	119	75	450	2	4	Fuel	16.6	1.5	33.2
571	119	30	.4	119	120	76	443	4	2	Fuel	1.4	1.0	27.5
583	121	85	.5	120	121	84	444	4	3	Fuel	13.3	1.1	35.6
483	120	98	.5	119	120	69	454	4	4	Fuel	27.9	1.4	41.9
532	122	b70	c.4	122	123	(a)	447	4	4	Fuel	24.6	1.8	46.2
570	119	d39	.5	119	118	(a)	449	6	2	Fuel	12.0	1.2	33.3
487	120	93	.4	120	120	87	448	6	3	Fuel	22.9	2.0	38.1
488	120	b68	c.3	120	120	84	449	8	2	Fuel	15.4	.4	26.6
486	120	b96	c.5	120	120	70	453	8	3	Oxidant	.4	1.0	37.4
481	120	123	.5	120	120	80	443	8	4	Oxidant	20.8	1.4	55.8

<sup>a</sup>No record obtained.<sup>b</sup>Peak pressure; maximum pressure possible was probably not attained.<sup>c</sup>Time to attain peak combustion-chamber pressure.<sup>d</sup>Leak in line to recording instrument.

TABLE IV. - SUMMARY OF IGNITION DATA AT 68° F AND SEA-LEVEL PRESSURE FOR A DIALLYLANILINE-  
TRIETHYLAMINE MIXTURE AND RED FUMING NITRIC ACID  
[0.2-In.-diameter exhaust nozzle.]

Run	Average propellant temperature, °F	Maximum combustion-chamber pressure, lb/sq in. gage	Time to attain maximum combustion-chamber pressure, sec	Temperature, °F			Propellant-injection pressure, lb/sq in. gage	Combustion-chamber length, in.	Combustion-chamber diameter, in.	Lead propellant into combustion chamber	Time between jet entries into combustion chamber, millsec	Time between ignition and normal combustion picture, millsec	Ignition delay, millsec
				Oxidant	Fuel	Ambient air							
669	69	354	1.0	69	69	71	446	1	1	Fuel	7.6	0.3	3.5
670	69	357	1.1	69	70	75	445	1	2	Fuel	2.4	.2	9.1
671	69	a 289	b .4	69	69	77	450	1	3	Fuel	4.7	.2	11.2
672	68	a 136	b .5	68	68	71	448	1	4	Fuel	6.8	1.2	15.0
673	68	(c)	(c)	68	68	72	447	2	1	Oxidant	2.5	.2	6.0
713	68	372	.9	68	69	76	447	2	1	Fuel	2.2	.4	6.4
695	68	a 306	b .4	68	67	70	443	2	2	Fuel	8.1	.5	11.1
692	69	{c}	{c}	69	68	89	448	2	3	Fuel	4.8	.5	19.6
707	68	{c}	{c}	68	68	75	447	2	3	Fuel	6.7	.4	20.0
676	68	367	1.0	68	69	69	448	4	1	Fuel	19.3	.2	6.2
675	68	{c}	{c}	68	68	72	452	4	2	Fuel	4.3	1.1	15.0
694	68	{c}	{c}	68	67	78	445	4	3	Fuel	6.3	.2	29.7
712	68	a 164	b .3	68	68	85	443	4	4	Oxidant	23.8	1.2	37.5
677	68	376	.9	69	68	71	443	6	1	Fuel	26.1	.5	6.6
678	68	{c}	{c}	68	68	71	449	6	2	Oxidant	5.6	1.6	20.0
715	68	414	.4	68	68	87	449	6	3	Fuel	148.5	1.3	28.0
681	67	{d}	{d}	67	68	71	447	6	3	Fuel	2.7	.5	38.0
696	69	a 324	b .3	69	68	70	443	6	4	Fuel	54.8	7.6	50.7
679	68	386	.8	69	67	67	449	8	1	Fuel	2.9	.6	8.2
718	68	{c}	{c}	68	69	(a)	445	8	2	Fuel	10.9	.7	22.1
710	68	{c}	{c}	68	68	76	449	8	3	Fuel	3.5	.8	41.9
683	71	a 200	b .5	73	69	81	443	8	4	Fuel	9.2	1.4	56.0

<sup>a</sup>Peak pressure; maximum pressure possible was probably not attained.

<sup>b</sup>Time to attain peak combustion-chamber pressure.

<sup>c</sup>Explosion occurred <2.5 millsec after ignition.

<sup>d</sup>Explosion occurred; time of occurrence difficult to determine.

TABLE V. - SUMMARY OF IGNITION DATA AT 0° F AND SEA-LEVEL PRESSURE FOR A DIALLYLANILINE-  
TRIETHYLAMINE MIXTURE AND RED FUMING NITRIC ACID  
[0.4-In.-diameter exhaust nozzle.]

Run	Average propellant temperature, °F	Maximum combustion-chamber pressure, lb/sq in. gage	Time to attain maximum combustion-chamber pressure, sec	Temperature, °F			Propellant injection pressure, lb/sq in. gage	Combustion-chamber length, in.	Combustion-chamber diameter, in.	Lead propellant into combustion chamber	Time between jet entries into combustion chamber, millisec	Time between ignition and normal combustion picture, millisec	Ignition delay, millisec
				Oxidant	Fuel	Ambient air							
460	-2	(a)	(a)	-2	-2	68	451	2	2	Oxidant	3.8	1.9	33.5
459	0	b207	c0.5	-1	0	68	439	2	3	(d)	<.2	.4	38.4
458	0	b197	c.5	0	0	66	446	2	4	Oxidant	5.6	2.3	43.1
457	1	304	0.4	1	2	66	448	4	2	Oxidant	0.3	1.0	24.1
427	0	308	.4	1	0	56	447	4	2	Oxidant	25.8	.8	33.5
529	-1	b212	c.5	-1	-1	65	444	4	3	Fuel	10.2	1.3	41.1
565	1	b213	c.5	1	2	(e)	442	4	4	Oxidant	7.8	1.7	49.7
454	-2	320	0.4	-2	-2	55	460	6	2	Oxidant	1.3	2.2	35.0
453	1	335	.3	1	1	59	453	6	3	Oxidant	1.2	1.6	36.5
452	1	350	.5	1	1	59	458	6	4	Oxidant	25.2	3.2	59.9
451	3	310	0.4	3	3	(e)	443	8	2	Oxidant	4.5	1.6	36.8
450	0	305	.3	-1	0	67	433	8	3	Oxidant	3.3	6.0	48.8
449	-2	342	.4	-2	-2	52	451	8	4	Fuel	5.0	1.5	75.5

<sup>a</sup>Explosion occurred 7 millisec after ignition.

<sup>b</sup>Peak pressure; maximum pressure possible was probably not attained.

<sup>c</sup>Time to attain peak combustion-chamber pressure.

<sup>d</sup>Both propellants entered combustion chamber in same motion-picture frame.

<sup>e</sup>No proper data.

TABLE VI. - SUMMARY OF IGNITION DATA AT -90° F AND SEA-LEVEL PRESSURE FOR A DIALLYLANILINE-  
TRIETHYLAMINE MIXTURE AND RED FUMING NITRIC ACID

Run	Average propellant temperature, °F	Maximum combustion-chamber pressure, lb/sq in. gage	Time to attain maximum combustion-chamber pressure, sec	Temperature, °F			Propellant-injection pressure, lb/sq in. gage	Combustion-chamber length, in.	Combustion-chamber diameter, in.	Lead propellant into combustion chamber	Time between jet entries into combustion chamber, millisecond	Time between ignition and normal combustion picture, millisecond	Ignition delay, millisecond
				Oxidant	Fuel	Ambient air							
0.2-In.-diameter exhaust nozzle													
545	-89	<sup>a</sup> 87	<sup>b</sup> 0.3	-88	-89	68	450	4	3	Oxidant	7.0	7.7	47.8
561	-89	<sup>a</sup> 213	<sup>b</sup> .4	-89	-89	66	442	4	4	Fuel	4.4	11.2	64.8
546	-93	190	.4	-92	-94	70	442	6	2	Oxidant	5.6	5.4	40.6
547	-89	300	.5	(c)	-89	76	443	6	3	Oxidant	4.3	9.8	50.1
542	-87	<sup>a</sup> 128	<sup>b</sup> .3	-89	-84	60	448	8	4	Fuel	10.4	2.8	114
0.4-In.-diameter exhaust nozzle													
<sup>d</sup> 636	-92	231	0.6	-94	-90	46	445	2	2	Fuel	7.3	<sup>e</sup> 0.8	40.5
358	-90	<sup>a</sup> 280	<sup>b</sup> 2.2	-90	-90	72	452	2	2	Oxidant	20.1	1.7	43.8
<sup>d</sup> 637	-90	169	1.2	-90	-89	46	445	2	4	Fuel	7.0	3.2	53.1
442	-90	314	.6	-90	-90	62	452	2	4	Oxidant	60.2	4.3	80.5
577	-83	253	.5	-83	-83	63	445	4	2	Oxidant	2.6	1.8	51.7
432	-92	295	.5	-92	-91	48	446	4	3	Oxidant	40.2	5.0	59.3
576	-89	(f)	(f)	-89	(c)	(c)	446	4	4	Oxidant	1.5	1.7	84.5
434	-89	302	.4	-89	-88	57	450	6	3	Oxidant	17.0	13.3	54.3
356	-89	<sup>a</sup> 226	<sup>b</sup> .4	-89	-89	65	443	6	4	Oxidant	41.6	5.0	87.7
437	-90	308	.4	-91	-90	53	451	8	2	Oxidant	55.0	10.9	45.5
<sup>d</sup> 635	-91	260	.8	-92	-90	48	448	8	2	Fuel	6.5	3.9	53.1
438	-89	307	.2	-89	-89	48	446	8	3	Oxidant	30.7	19.9	66.8
467	-90	322	.2	-90	-89	60	449	8	4	Fuel	3.1	18.0	98.7
0.8-In.-diameter exhaust nozzle													
504	-90	63	0.3	-90	-90	53	448	6	2	Oxidant	3.9	8.5	88.7
503	-90	84	.5	-90	-90	56	446	6	3	Oxidant	1.1	5.1	106
505	-90	60	.4	-90	-90	51	446	8	2	Oxidant	4.9	5.7	60.0

<sup>a</sup>Peak pressure; maximum pressure possible was probably not attained.

<sup>b</sup>Time to attain peak combustion-chamber pressure.

<sup>c</sup>No proper data.

<sup>d</sup>Run made with two-on-one injector.

<sup>e</sup>Nondestructive explosion occurred 4 millisecond after ignition.

<sup>f</sup>Explosion destroyed chamber; time of occurrence difficult to determine.

TABLE VII. - SUMMARY OF IGNITION DATA AT SEVERAL TEMPERATURES AND A PRESSURE ALTITUDE OF 90,000 FEET FOR A DIALLYLANILINE-  
TRIETHYLAMINE MIXTURE AND RED FUMING NITRIC ACID

Run	Average propellant temperature, °F	Maximum combustion-chamber pressure, lb/sq in. gage	Time to attain maximum combustion-chamber pressure, sec	Temperature, °F			Propellant-injection pressure, lb/sq in. gage	Combustion-chamber length, in.	Combustion-chamber diameter, in.	Lead propellant into combustion chamber	Time between jet entries into combustion chamber, millisecond	Time between ignition and normal combustion picture, millisecond	Ignition delay, millisecond
				Oxidant	Fuel	Ambient air							
0.2-In.-diameter exhaust nozzle													
541	119	225	0.5	120	118	{a}	446	2	2	Fuel	27.6	0.5	7.1
540	120	145	.4	119	121	{a}	447	4	2	Fuel	.5	.8	11.5
522	119	365	.3	119	119	{a}	451	6	2	Fuel	13.4	.4	17.0
568	120	243	1.0	120	119	{a}	447	8	2	Fuel	50.5	.7	12.3
595	119	{a}	{a}	119	119	88	444	8	2	Fuel	2.3	1.1	24.7
598	119	{b}	{b}	118	120	90	453	8	4	Fuel	20.4	1.3	42.2
0.4-In.-diameter exhaust nozzle													
472	120	296	0.6	120	120	82	448	2	2	Fuel	25.4	0.3	7.3
471	120	305	.5	119	120	80	446	8	2	Fuel	16.2	.5	16.2
473	-90	243	.8	-90	-90	64	459	2	2	Fuel	11.5	.6	44.6
0.8-In.-diameter exhaust nozzle													
510	120	45	0.4	120	120	72	451	2	2	Fuel	1.8	0.4	32.5
511	119	108	.8	119	120	65	447	2	4	Fuel	4.4	1.0	35.4
513	120	63	.7	120	120	69	451	8	2	Fuel	19.3	.9	33.9
509	-91	<sup>c</sup> 66	<sup>d</sup> .5	-91	-91	44	451	2	4	Fuel	0.7	5.4	329
507	-90	(a)	(a)	-90	(a)	47	449	8	2	Oxidant	19.5	3.2	316
539	-90	<sup>c</sup> 10	<sup>d</sup> .1	-90	-89	(a)	448	8	2	Oxidant	7.2	4.1	317
506	-90	87	.5	-90	-90	55	447	8	4	Oxidant	11.5	3.1	297

<sup>a</sup>No record.

<sup>b</sup>Explosion destroyed chamber 9 millisecond after ignition.

<sup>c</sup>Peak pressure; maximum pressure possible was probably not attained.

<sup>d</sup>Time to attain peak combustion-chamber pressure.

TABLE VIII. - SUMMARY OF IGNITION DATA AT 120° F AND SEA-LEVEL PRESSURE FOR A DIALYL ANILINE-TRIETHYLAMINE MIXTURE AND RED FUMING NITRIC ACID IN COMBUSTION CHAMBERS WITH VARIOUS INNER-WALL SURFACES  
 [4-in.-long, 2-in.-inside-diameter combustion chamber; 0.4-in.-diameter exhaust nozzle.]

Run	Average propellant temperature, °F	Maximum combustion-chamber pressure, lb/sq in. gage	Time to attain maximum combustion-chamber pressure, sec	Temperature, °F			Propellant-injection pressure, lb/sq in. gage	Lead propellant into combustion chamber	Time between jet entries into combustion chamber, millsec	Time between ignition and normal combustion picture, millsec	Ignition delay, millsec
				Oxidant	Fuel	Ambient air					
Smooth											
656	120	<sup>a</sup> 254	b <sub>1.5</sub>	120	120	79	447	Fuel	20.0	0.2	14.8
655	120	<sup>a</sup> 251	b <sub>1.6</sub>	120	120	78	447	Fuel	22.0	.4	15.2
654	120	<sup>a</sup> 224	b <sub>1.5</sub>	119	120	76	447	Fuel	17.9	.3	15.4
Screw threaded											
627	121	295	0.7	121	121	73	451	Fuel	25.3	0.5	11.0
628	120	290	.8	119	120	73	449	Fuel	2.6	.2	21.3
643	120	255	1.4	120	121	75	448	Oxidant	4.3	.5	17.4
644	120	<sup>a</sup> 269	b <sub>1.5</sub>	120	121	76	447	Fuel	3.7	.5	19.6
645	120	246	1.4	120	121	76	449	Fuel	25.2	.5	12.7
646	120	<sup>a</sup> 254	b <sub>1.5</sub>	119	120	75	450	Fuel	54.1	.8	11.4
647	120	<sup>a</sup> 248	b <sub>1.5</sub>	120	120	75	449	Oxidant	12.9	1.3	17.9
648	120	{c}	{c}	120	121	73	447	Oxidant	.9	.5	18.9
649	120	{c}	{c}	119	121	71	448	Fuel	54.7	.6	9.7
650	120	<sup>a</sup> 291	b <sub>1.5</sub>	120	120	67	449	Fuel	29.9	.6	11.2
651	120	<sup>a</sup> 297	b <sub>1.5</sub>	119	120	73	448	Fuel	30.3	.7	11.9
652	120	(d)	(d)	119	121	76	449	Fuel	1.8	.4	18.5
653	120	<sup>a</sup> 261	b <sub>1.5</sub>	120	121	72	447	Fuel	19.1	.5	11.2
Sand blasted											
630	119	290	0.9	118	121	78	453	Fuel	9.6	0.2	16.2
Finned											
610	121	(d)	(d)	121	120	82	447	Fuel	3.1	0.6	17.7
611	120	<sup>a</sup> 66	b <sub>1.7</sub>	120	120	85	444	Fuel	4.2	.5	18.9
631	120	290	.7	120	121	70	449	Fuel	12.5	1.0	15.0
632	120	(d)	(d)	120	120	77	446	Fuel	2.1	.9	21.4
633	120	(d)	(d)	119	121	69	448	Fuel	.8	.5	23.1
665	120	(d)	(d)	120	120	71	448	Fuel	21.7	.3	18.5
666	120	(d)	(d)	120	121	74	451	Fuel	27.6	.6	19.2
667	120	<sup>a</sup> 276	b <sub>1.5</sub>	120	120	82	450	Fuel	3.2	.3	17.1
668	120	(d)	(d)	120	120	73	448	Fuel	6.0	.5	19.6
690	119	<sup>a</sup> 267	b <sub>1.6</sub>	119	120	77	450	Fuel	.5	.5	19.8
691	120	(d)	(d)	119	121	82	449	Fuel	1.8	.4	23.2

<sup>a</sup>Peak pressure; maximum pressure possible was probably not attained.

<sup>b</sup>Time to attain peak combustion-chamber pressure.

<sup>c</sup>No proper record.

<sup>d</sup>Explosion occurred <2.5 millisec after ignition.

TABLE IX. - SUMMARY OF IGNITION DATA AT 40° F AND SEA-LEVEL PRESSURE FOR A DIALLYLANILINE-  
TRIETHYLAMINE MIXTURE AND RED FUMING NITRIC ACID

[5-In.-long, 2-in.-inside-diameter combustion chamber; 0.3-in.-diameter exhaust nozzle.]

Run	Average propellant temperature, °F	Maximum combustion-chamber pressure, lb/sq in. gage	Time to attain maximum combustion-chamber pressure, sec	Temperature, °F				Propellant-injection pressure, lb/sq in. gage	Lead propellant into combustion chamber	Time between jet entries into combustion chamber, millsec	Time between ignition and normal combustion picture, millsec	Ignition delay, millsec
				Oxidant	Fuel	Constant temperature bath	Ambient air					
725	39	360	0.7	39	39	40	67	449	Fuel	10.0	0.6	19.3
726	39	350	.7	39	39	40	62	450	Fuel	5.1	.5	23.4
727	39	(a)	(a)	39	40	40	67	450	Oxidant	3.4	.4	25.9
728	40	354	.7	41	40	39	64	443	Oxidant	6.6	.7	28.4
729	40	350	.8	40	39	39	65	447	Fuel	(b)	(b)	(b)
730	40	348	1.0	41	40	39	60	447	Oxidant	5.1	.5	27.0
731	40	365	.8	40	40	39	55	443	Fuel	4.5	.8	24.0
732	40	(a)	(a)	40	40	39	58	449	(c)	<.2	.8	27.1

<sup>a</sup>Explosion occurred 2 millsec after ignition.

<sup>b</sup>No timing marks on film.

<sup>c</sup>Both propellants entered combustion chamber in same motion-picture frame.

TABLE X. - SUMMARY OF IGNITION DATA AT SEVERAL TEMPERATURES AND SEA-LEVEL PRESSURE FOR TRIETHYL TRITHIOPHOSPHITE AND RED FUMING NITRIC ACID  
 [0.4-In.-diameter exhaust nozzle.]

Run	Average propellant temperature, °F	Maximum combustion-chamber pressure, lb/sq in. gage	Time to attain maximum combustion-chamber pressure, sec	Temperature, °F			Propellant injection pressure, lb/sq in. gage	Combustion-chamber length, in.	Combustion-chamber diameter, in.	Lead propellant into combustion chamber	Time between jet entries into combustion chamber, millisecond	Time between ignition and normal combustion picture, millisecond	Ignition delay, millisecond
				Oxidant	Fuel	Ambient air							
550	120	<sup>a</sup> 187	<sup>b</sup> 0.5	120	120	82	447	2	2	Fuel	6.1	0.9	3.8
553	118	205	.7	119	117	86	445	2	4	Fuel	11.9	3.1	6.0
<sup>c</sup> 258	121	220	.5	121	121	78	445	4	2	Oxidant	8.7	1.0	2.1
557	120	243	.5	119	121	89	443	8	2	Fuel	2.6	2.3	4.3
556	119	241	.7	119	118	88	453	8	4	Fuel	10.4	5.7	13.2
575	-90	220	0.7	-90	-90	64	443	2	2	Fuel	1.7	1.6	8.3
<sup>c</sup> 255	-95	182	.5	-94	-95	63	441	4	2	Fuel	4.1	.8	4.9
574	-89	280	.6	(d)	-89	56	448	8	2	Fuel	12.1	10.2	5.0
555	-90	177	.6	-90	-90	69	443	8	2	Oxidant	3.8	7.3	8.0

<sup>a</sup>Peak pressure; maximum pressure possible was probably not attained.

<sup>b</sup>Time to attain peak combustion-chamber pressure.

<sup>c</sup>From ref. 7.

<sup>d</sup>No proper record.

TABLE XI. - VARIATION IN IGNITION DELAY DUE TO DIFFERENCES IN PRESSURE ALTITUDE

Run		Approximate propellant temperature, °F	Exhaust-nozzle diameter, in.	Combustion-chamber length, in.	Combustion-chamber diameter, in.	Ignition delay, millisec		
Sea-level	90,000 Feet					Sea-level	90,000 Feet	Difference (a)
520	541	120	.2	2	2	8	7	S
549	540	120	.2	4	2	14	12	S
548	522	120	.2	6	2	17	17	S
697	568	120	.2	8	2	15	12	S
514	598	120	.2	8	4	39	42	S
642	472	120	.4	2	2	9	7	S
445	471	120	.4	8	2	17	16	S
452	473	-90	.4	2	2	44	45	S
573	510	120	.8	2	2	27	33	M
492	511	120	.8	2	4	17	35	M
488	513	120	.8	8	2	15	34	M
(b)	509	-90	.8	2	4	c153	329	L
446	507	-90	.8	8	2	60	316	L
446	539	-90	.8	8	2	60	317	L
(b)	506	-90	.8	8	4	c114	297	L

<sup>a</sup>Small difference (within experimental error), S.

Significant difference (~10 to 20 millisec), M.

Large difference (&gt;150 millisec), L.

<sup>b</sup>No actual data.<sup>c</sup>Obtained by extrapolation of other data.

TABLE XIII. - COMPARISON OF IGNITION AND OTHER DATA FOR VARIOUS TYPES OF COMBUSTION CHAMBERS

Chamber type (4-in.-long; 2-in.-I.D.)	Inner-surface area of plastic cylinder, sq in.		Total inner-surface area of combustion chamber with 0.4-inch-diameter exhaust nozzle, $A_t$ , sq in.		Effective nozzle area, $A_n^*$ sq in.	Effective surface area, $A_t^*$ sq in.	Combustion- chamber volume, cu in.	Ignition delay, millisec	
	Actual	Relative	Actual	Relative				Experimental <sup>a</sup>	Calculated <sup>b</sup>
Smooth walled	23.6	1	30.5	1	9.3	39.8	11.8	15.1	15.7
Screw threaded	32.8	1.4	39.6	1.3	9.3	48.9	11.8	14.8	19.3
Sand blasted	42.2	1.8	49.0	1.6	9.3	58.3	11.8	16.2	23.0
Finned	61.5	2.6	68.4	2.2	9.3	77.7	11.5	19.4	30.7

<sup>a</sup>Average values at 120° F.<sup>b</sup>From eq. (4) at 120° F.

TABLE XIII. - COMPARISON OF IGNITION DATA AT 120° F OF ONE-  
ON-ONE AND TWO-ON-ONE INJECTION SYSTEMS

[0.4-In.-diameter exhaust nozzle.]

Run	Combustion-chamber length, in.	Combustion-chamber diameter, in.	Ignition delay, millisecond	
			One-on-one injector	Two-on-one injector
622	1	1	6.4	----
659	1	1	----	6.3
357	2	2	12.9	----
614	2	2	----	13.1
463	8	2	26.4	----
634	8	2	----	25.0
447	8	4	48.3	----
612	8	4	----	48.4

TABLE XIV. - COMPARISON OF IGNITION DATA FOR TWO FUELS

[0.4-In.-diameter exhaust nozzle.]

Amine <sup>a</sup>	Run	Thiophos-phite <sup>b</sup>	Approximate propellant temperature, °F	Combustion-chamber length, in.	Combustion-chamber diameter, in.	Average ignition delay, millisec	
						Amine <sup>a</sup>	Thiophos-phite <sup>b</sup>
357,614, 642		550	120	2	2	11.8	3.8
466		553	120	2	4	25.9	6.0
654,655, 656	c 258	258	120	4	2	15.1	2.1
445,463, 634		557	120	8	2	22.9	4.3
447,594, 612		556	120	8	4	48.3	13.2
358,636		575	-90	2	2	42.2	8.3
445	c 255	255	-90	4	2	51.7	4.9
437,635		555,574	-90	8	2	49.3	6.5

<sup>a</sup>53 Percent diallylaniline and 43 percent triethylamine by weight.<sup>b</sup>Triethyl trithiophosphite.<sup>c</sup>From ref. 7.

TABLE XV. - COMPARISON OF IGNITION DATA FOR COMBUSTION CHAMBERS WITH SIMILAR EFFECTIVE SURFACE AREAS

Run	Approximate propellant temperature, °F	Combustion-chamber length, in.	Combustion-chamber diameter, in.	Exhaust-nozzle diameter, in.	Total inner-surface area of combustion chamber, $A_t^*$ , sq in.	Effective surface area, $A_t^*$ , sq in.	Average ignition delay, millisec
520	120	2	2	.2	18	21	8
584	120	4	1	.4	13	23	8
591,717	120	1	2	.4	12	26	11
586	120	6	1	.4	19	26	10
548	120	6	2	.2	43	45	17
465	120	2	3	.4	31	44	17
524	120	2	4	.2	48	51	18
588	120	1	4	.4	35	49	19
569,697 445,463,634	120	8	2	.2	56	56	23
606	120	8	2	.4	56	58	23
353	120	4	3	.2	73	75	27
446	120	6	3	.4	69	75	25
491	120	4	4	.4	73	82	31
491	120	2	3	.8	31	82	28
515	120	8	3	.2	88	88	35
444	120	8	3	.4	88	90	35
583	120	4	3	.8	50	87	36
563	120	6	4	.2	98	99	38
486	120	8	3	.8	87	98	37
514,581 447,594,612	120	8	4	.2	123	123	51
514,581 447,594,612	120	8	4	.4	123	125	48
545	-90	4	3	.2	50	<sup>a</sup> 55	48
358,636	-90	2	2	.4	18	51	42
561	-90	4	4	.2	73	77	65
442,637	-90	2	4	.4	48	81	67

<sup>a</sup>Closely similar  $A_t^*$  values not available at -90° F.

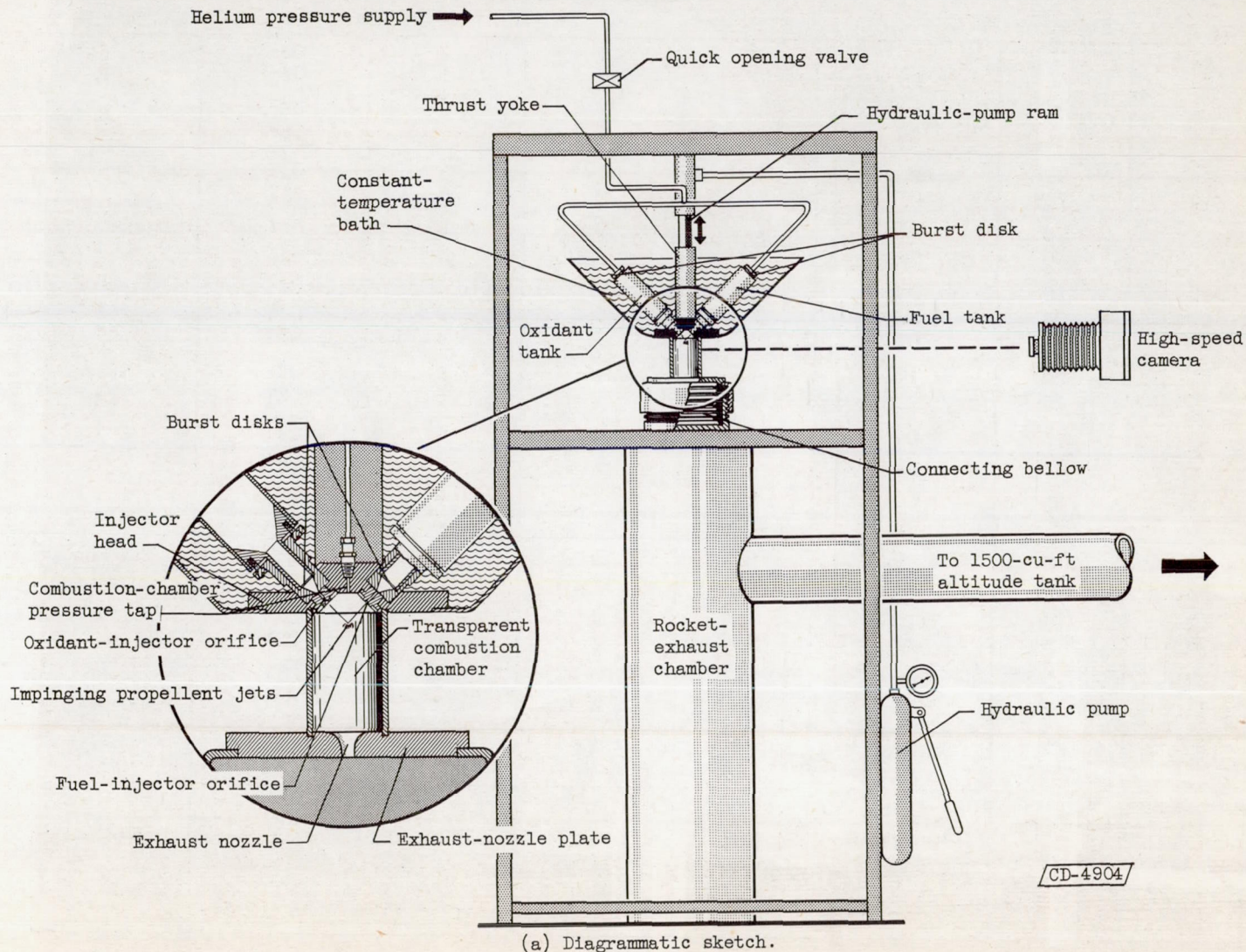
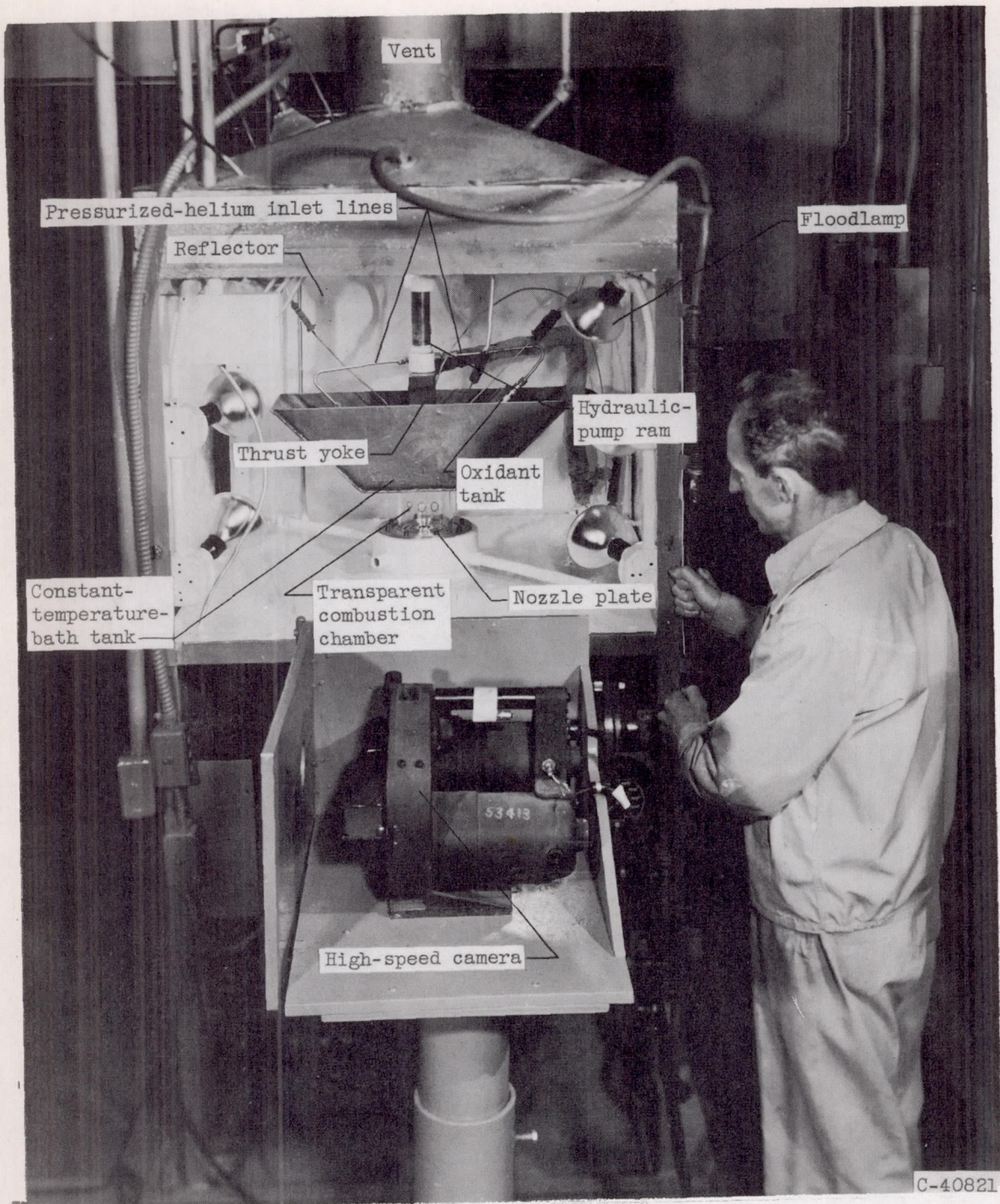
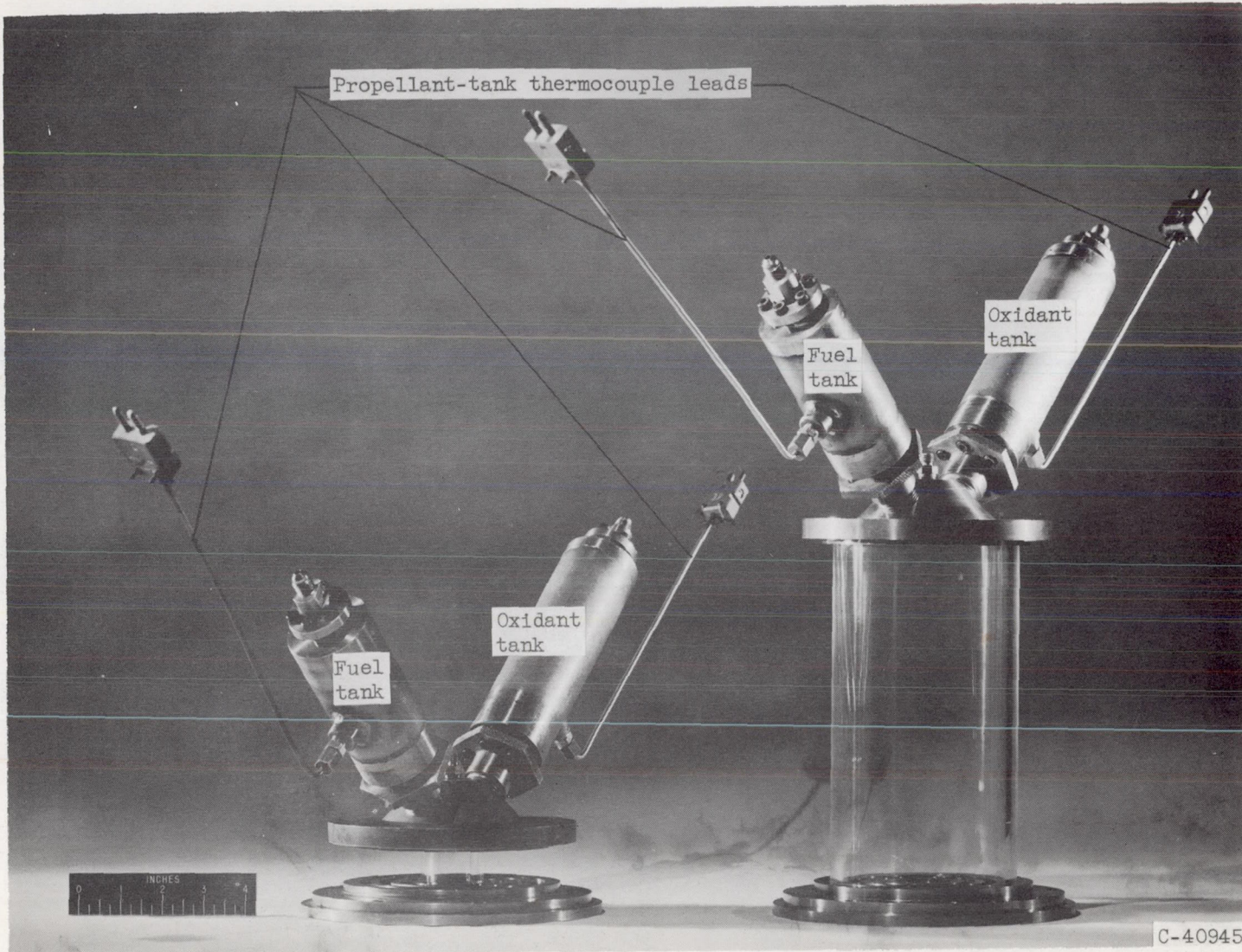


Figure 1. - Small-scale rocket-engine ignition-delay apparatus.



(b) Photograph of assembly.

Figure 1. - Small-scale rocket-engine ignition-delay apparatus.



(a) 1-Inch long with 1-inch inside diameter.

(b) 8-Inches long with 4-inch inside diameter.

Figure 2. - Comparison of two engine-assembly combustion-chamber sizes.

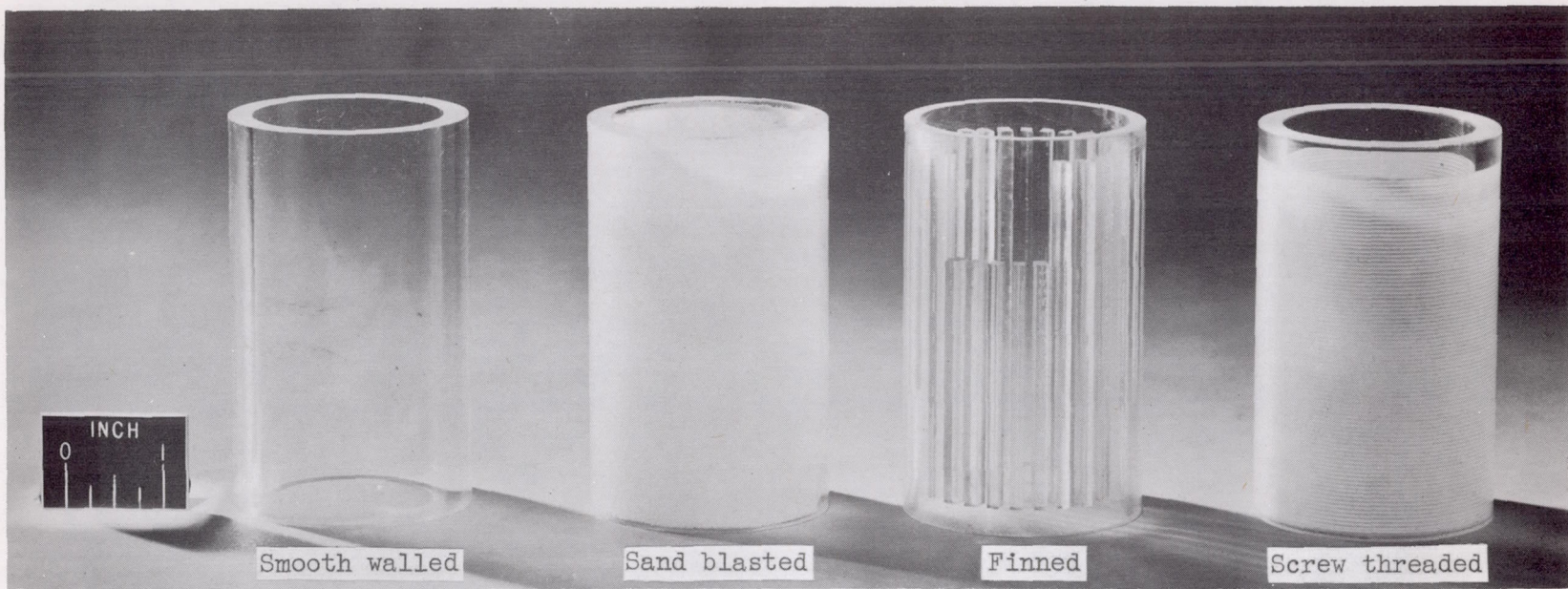


Figure 3. - Combustion-chamber cylinders with various types of inner surface.

C-40944

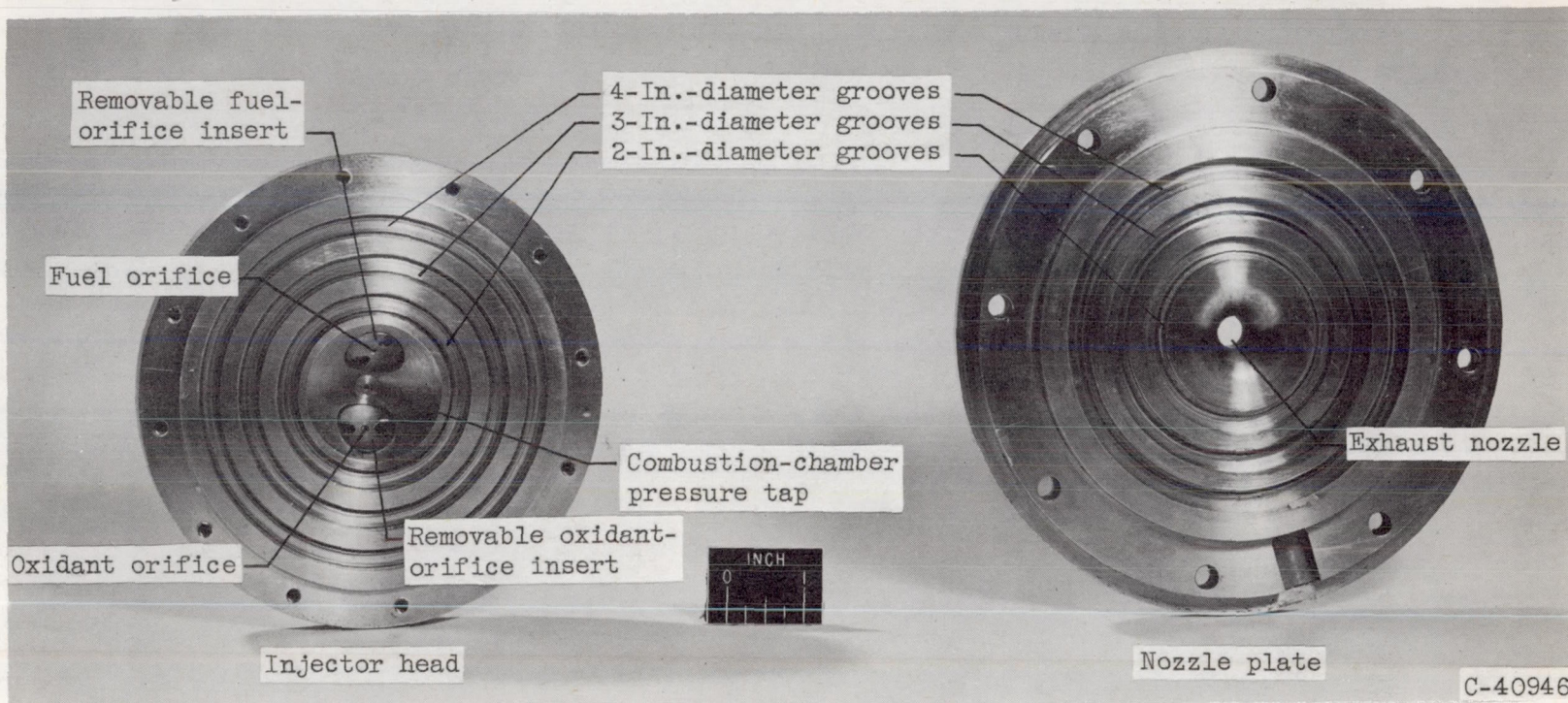


Figure 4. - Injector head and nozzle plate with 2-, 3-, and 4-inch-diameter combustion-chamber cylinders.

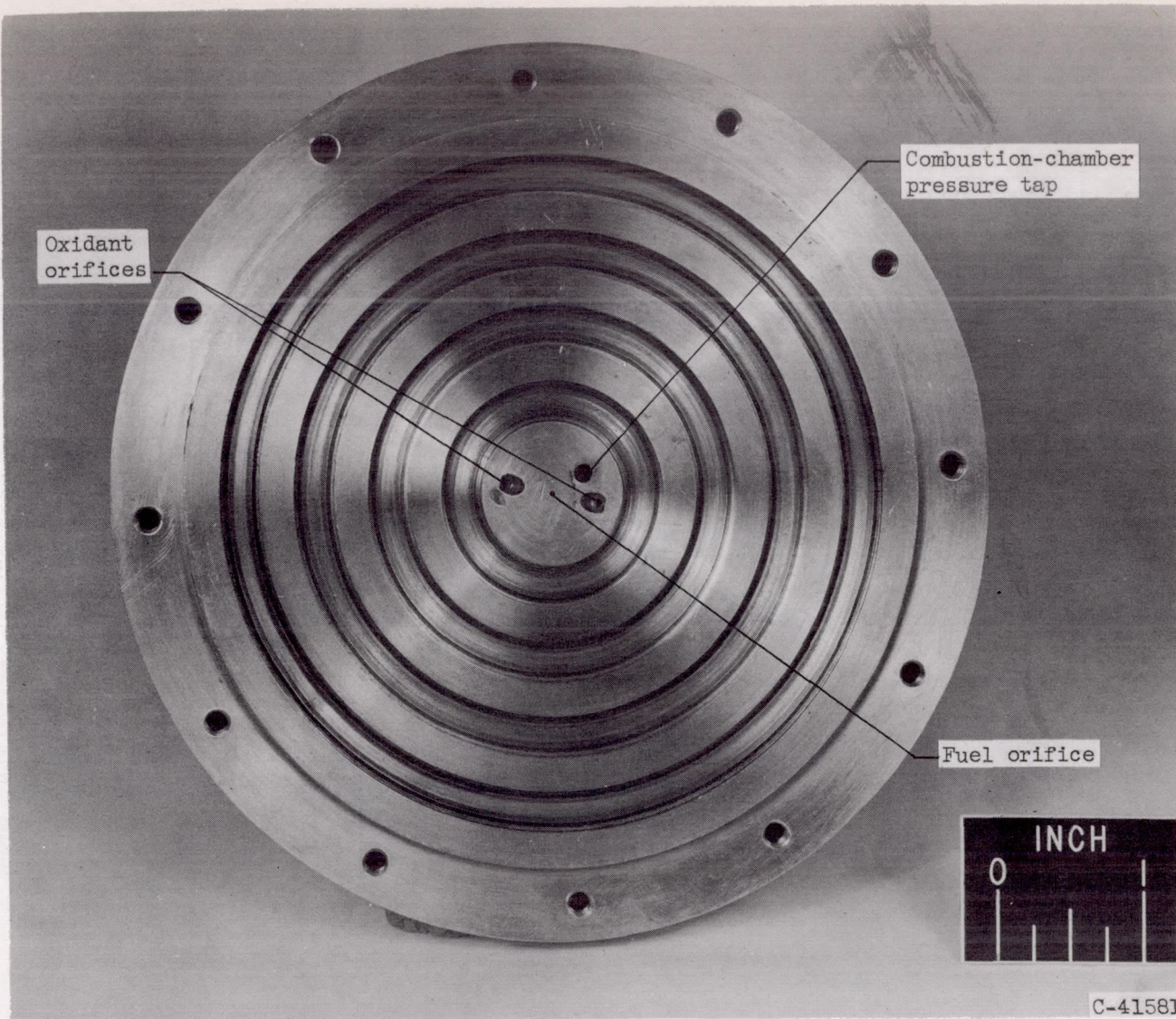


Figure 5. - Two-on-one injector head used in some auxiliary experiments.

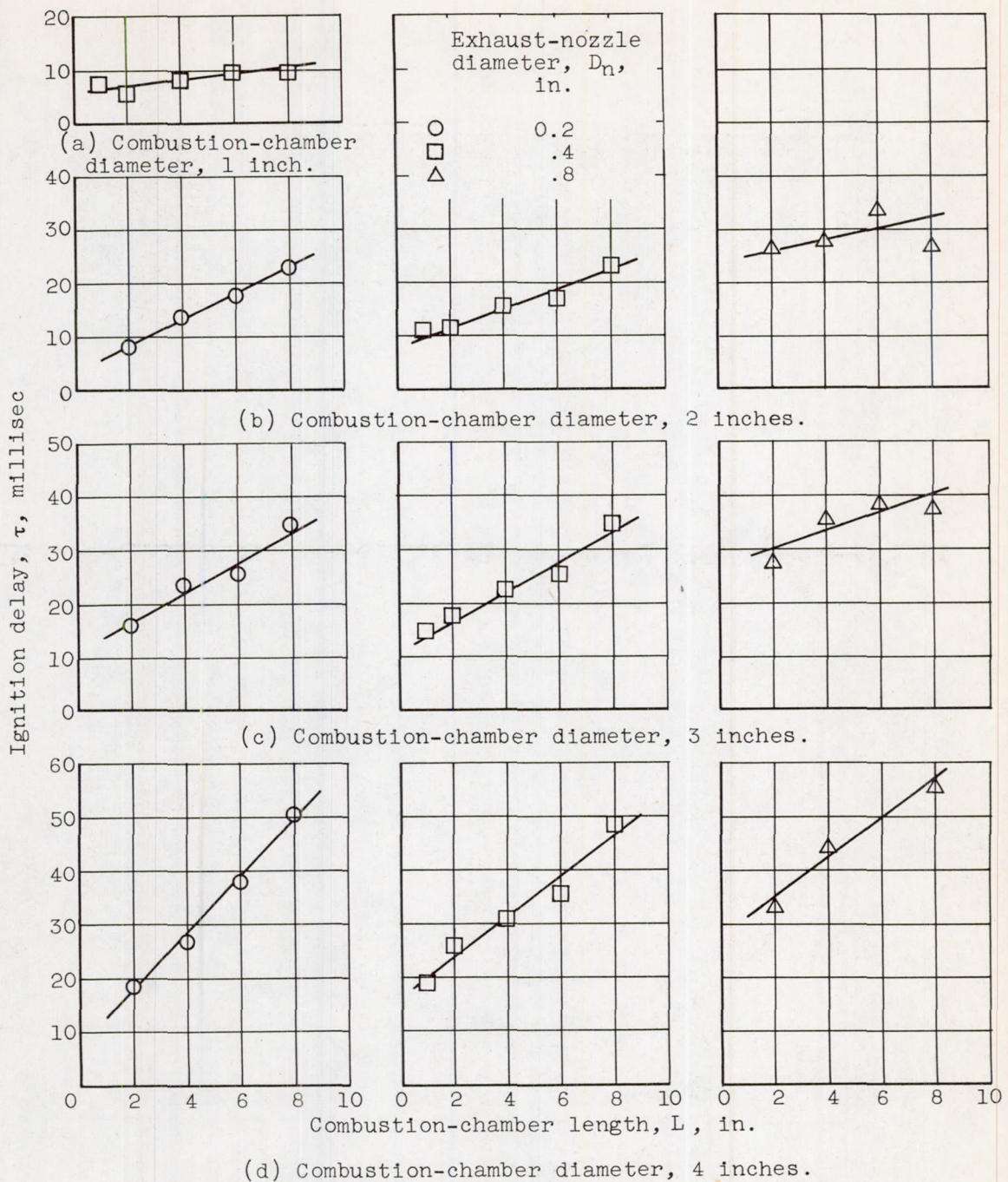


Figure 6. - Relation between average ignition delay and combustion-chamber length at 120° F and sea-level pressure for various chamber diameters and exhaust-nozzle diameters (diallylaniline-triethylamine mixture and red fuming nitric acid).

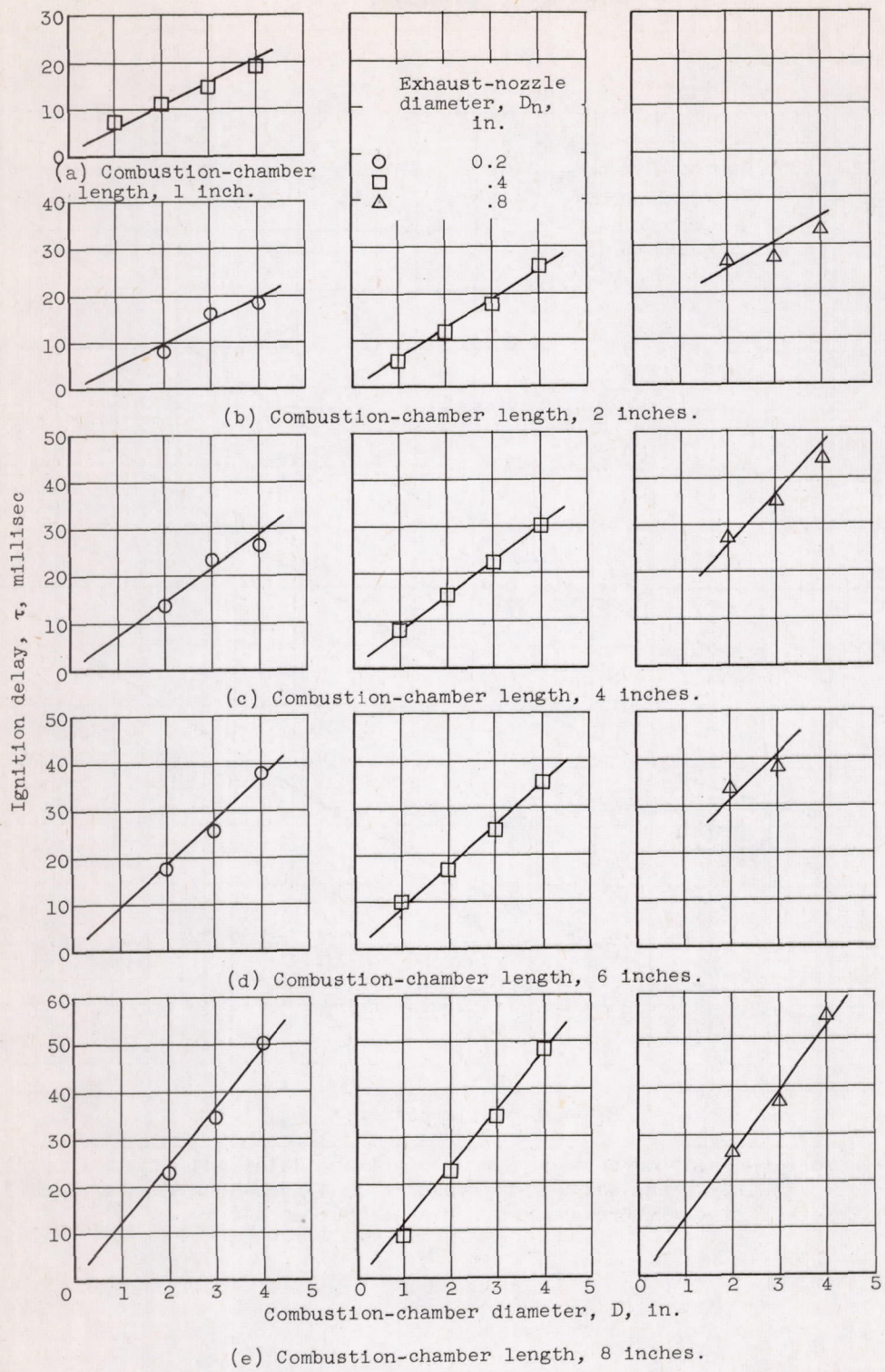


Figure 7. - Relation between average ignition delay and combustion-chamber diameter at 120° F and sea-level pressure for various combustion-chamber lengths and exhaust-nozzle diameters (diallylaniline-triethylamine mixture and red fuming nitric acid).

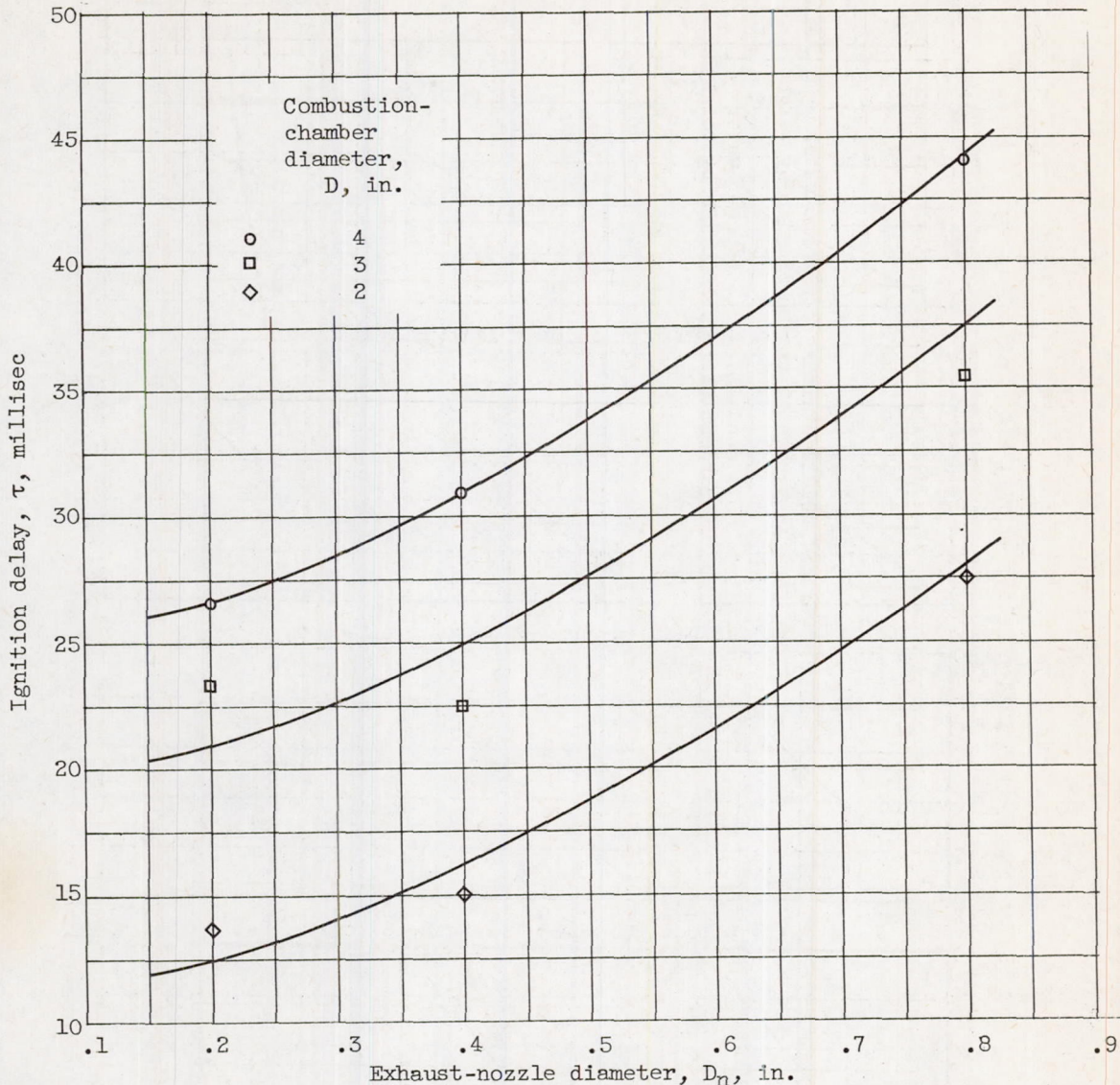


Figure 8. - Relation between average ignition delay and exhaust-nozzle diameter at 120° F and sea-level pressure for 4-inch-long chambers (diallylaniline-triethylamine mixture and red fuming nitric acid).

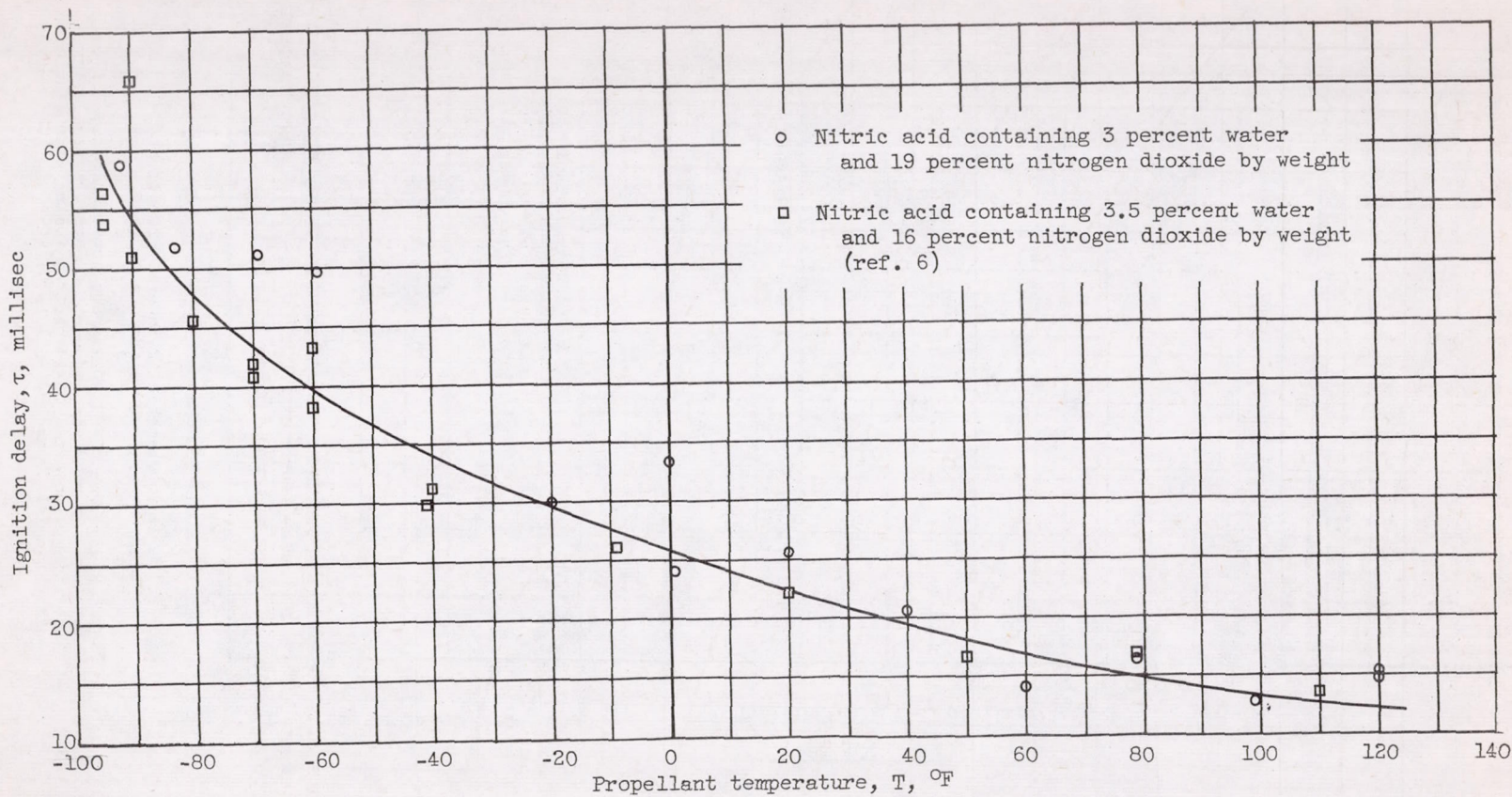


Figure 9. - Ignition delay of 57 percent diallylaniline and 43 percent triethylamine by weight and red fuming nitric acid (4-in.-long, 2-in.-inside-diameter combustion chamber; 0.4-in.-diameter exhaust nozzle).

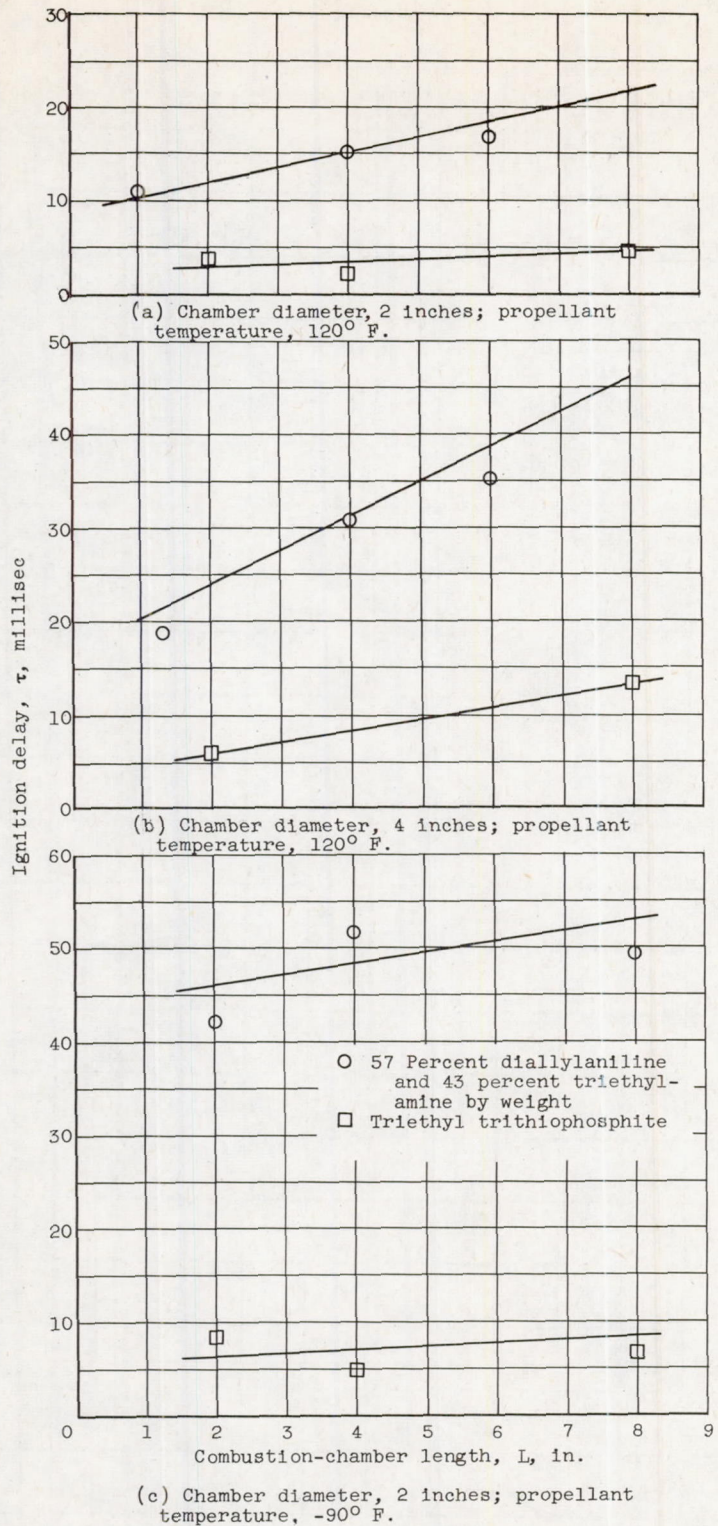


Figure 10. - Comparison of average ignition delays of two fuels in same size combustion chambers at similar operating conditions (oxidant, red fuming nitric acid; exhaust-nozzle diameter, 0.4 in.).

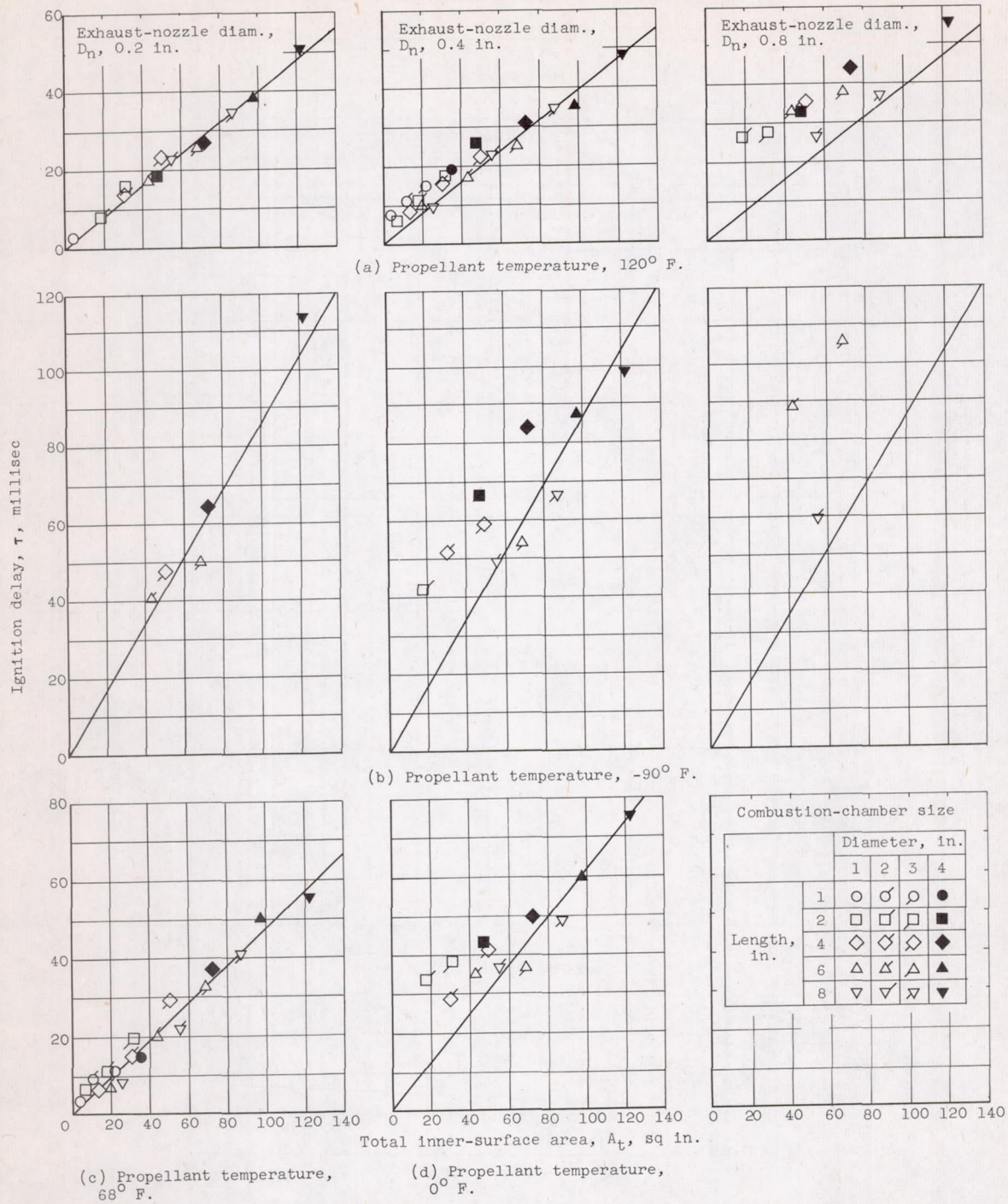


Figure 11. - Relation between ignition delay and total inner-surface area of combustion chamber (diallylaniline-triethylamine mixture and red fuming nitric acid).

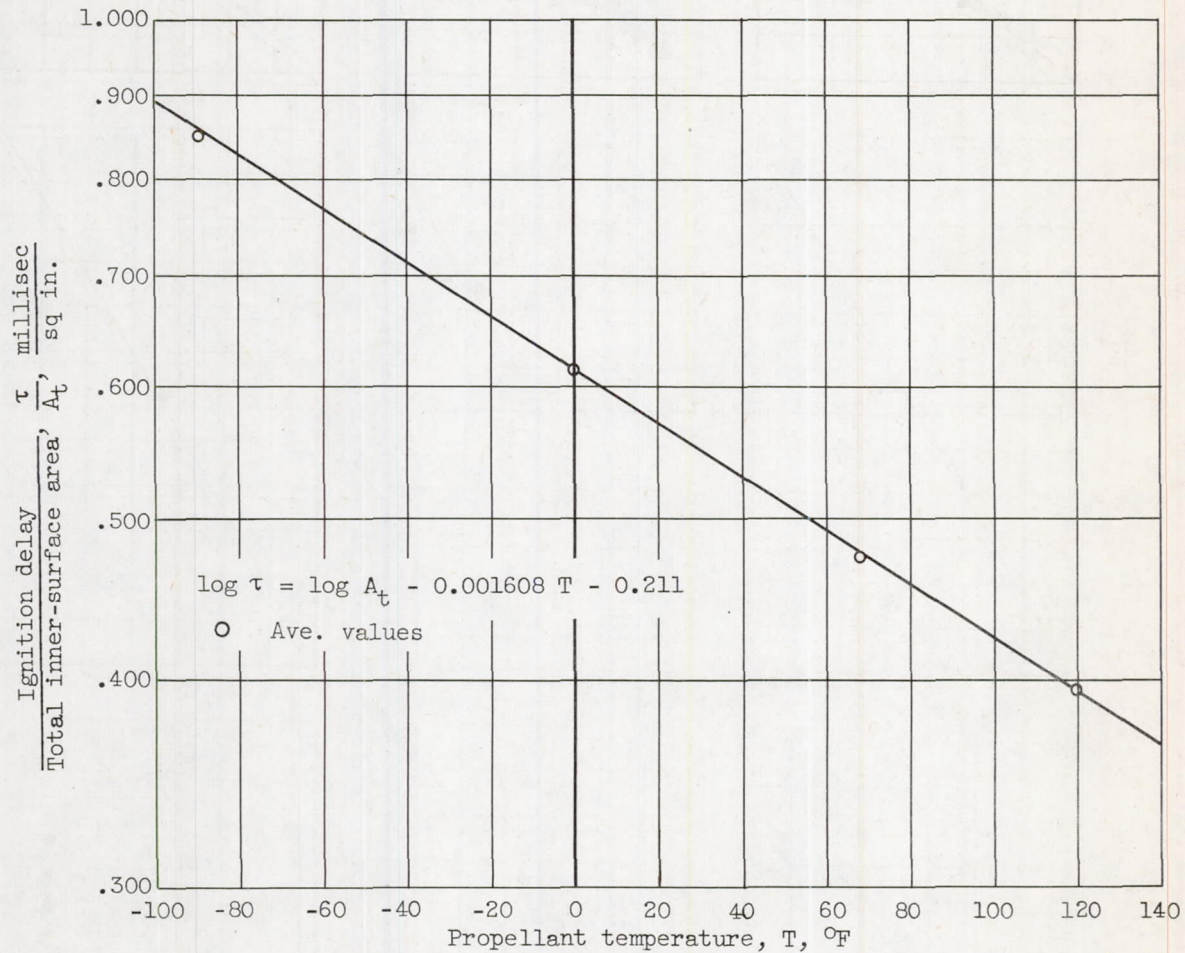


Figure 12. - Variation of ratio of ignition delay to total inner-surface area with propellant temperature (diallylaniline-triethylamine mixture and red fuming nitric acid).

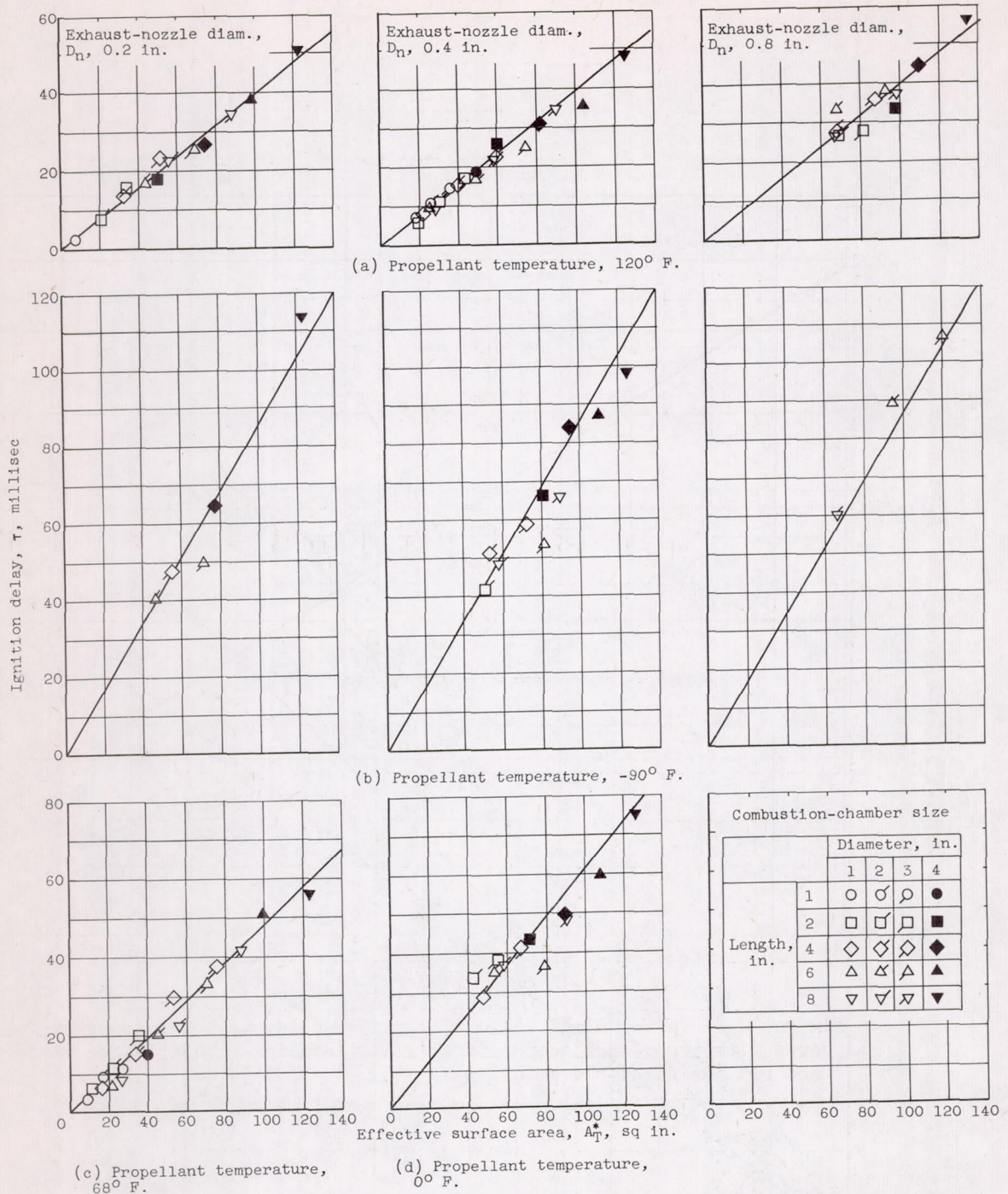
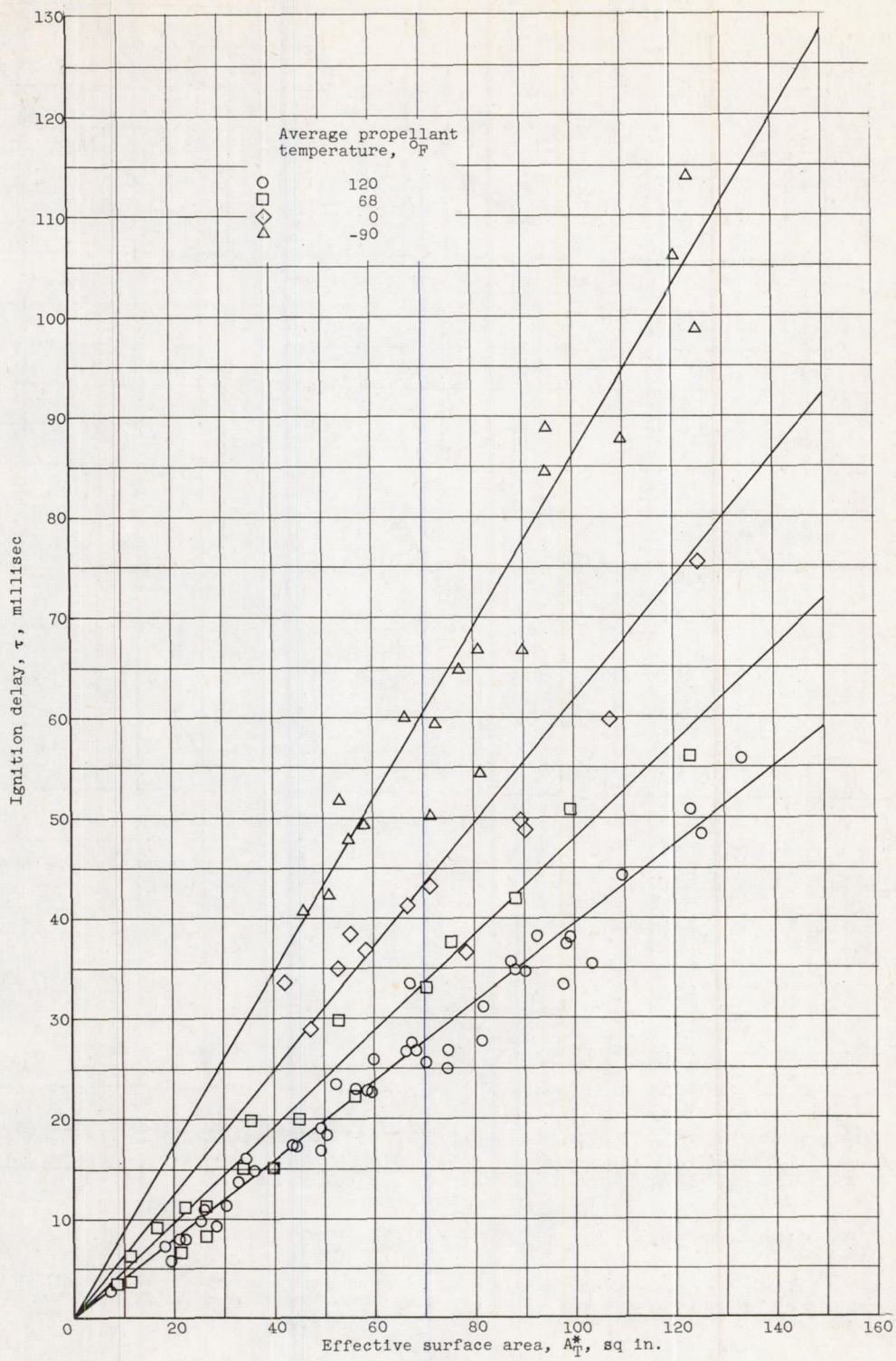


Figure 13. - Relation between ignition delay and effective surface area in individual and combined combustion-chamber configurations at various propellant temperatures (diallylaniline-triethylamine mixture and red fuming nitric acid).



(e) Combined plot.

Figure 13. - Concluded. Relation between ignition delay and effective surface area in individual and combined combustion-chamber configurations at various propellant temperatures (diallylaniline-triethylamine mixture and red fuming nitric acid).

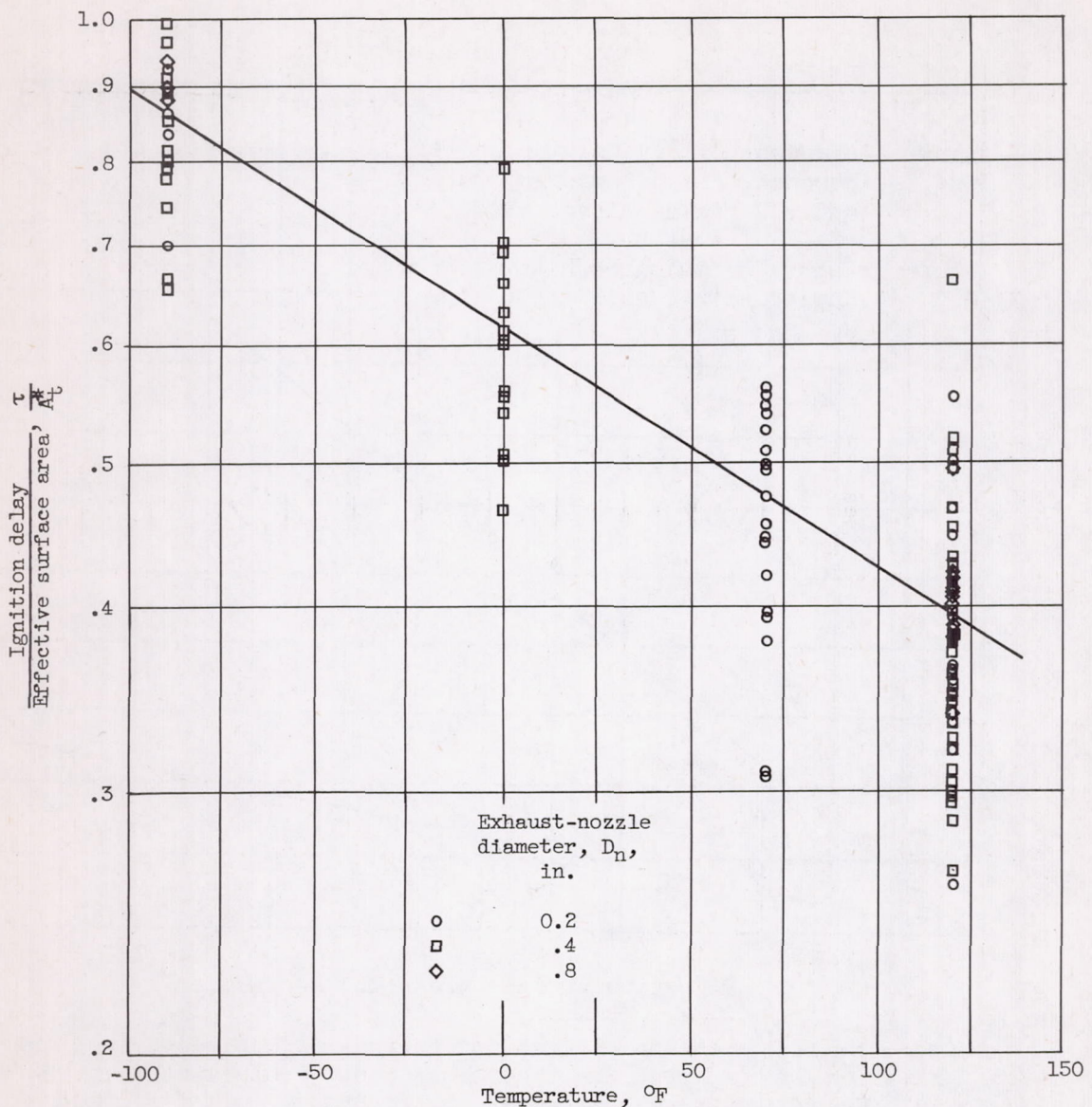


Figure 14. - Plot of equation (4) with data points from figure 13.

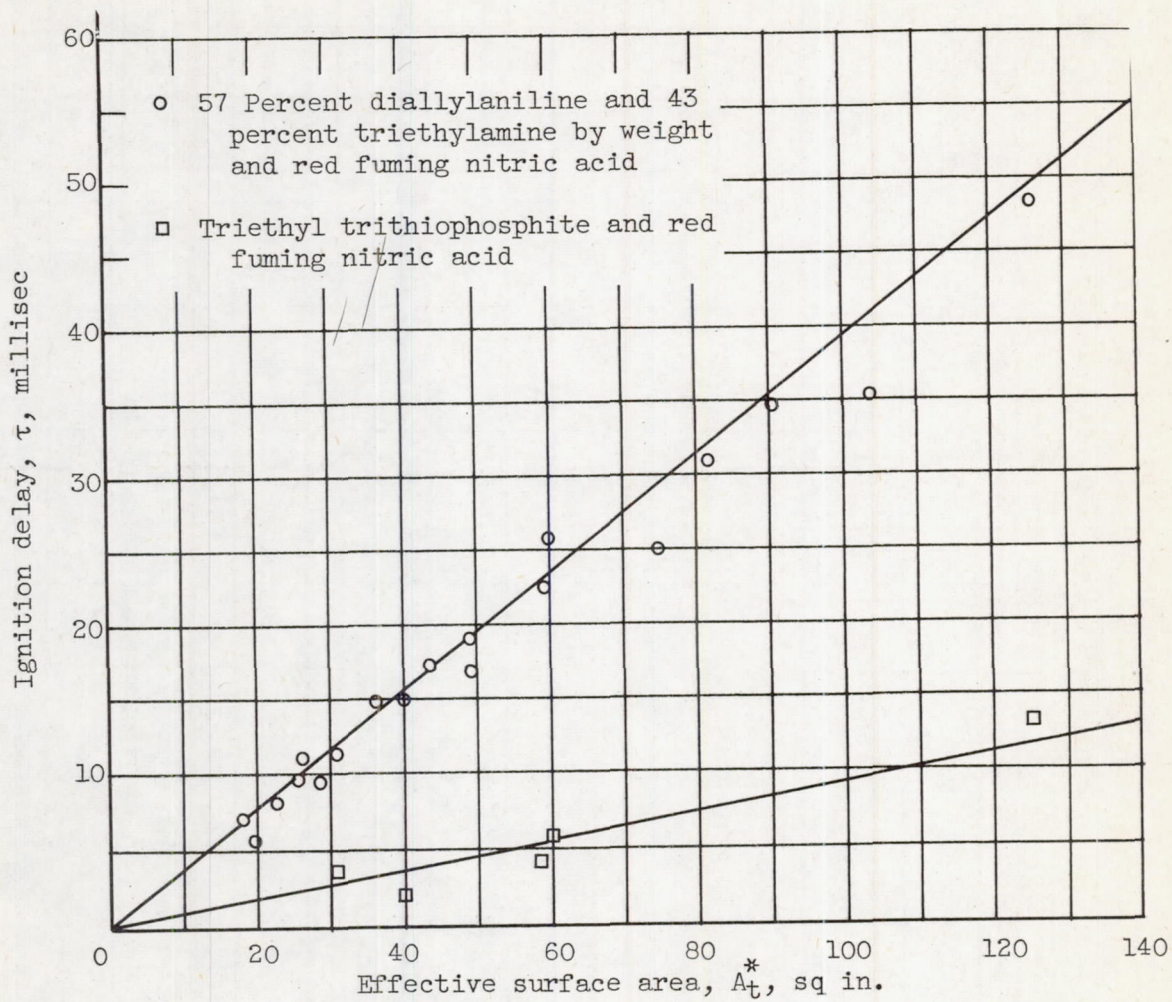


Figure 15. - Comparison of ignition delay - effective surface area relation for two propellant combinations. Propellant temperature, 120° F; exhaust-nozzle diameter, 0.4 inch.

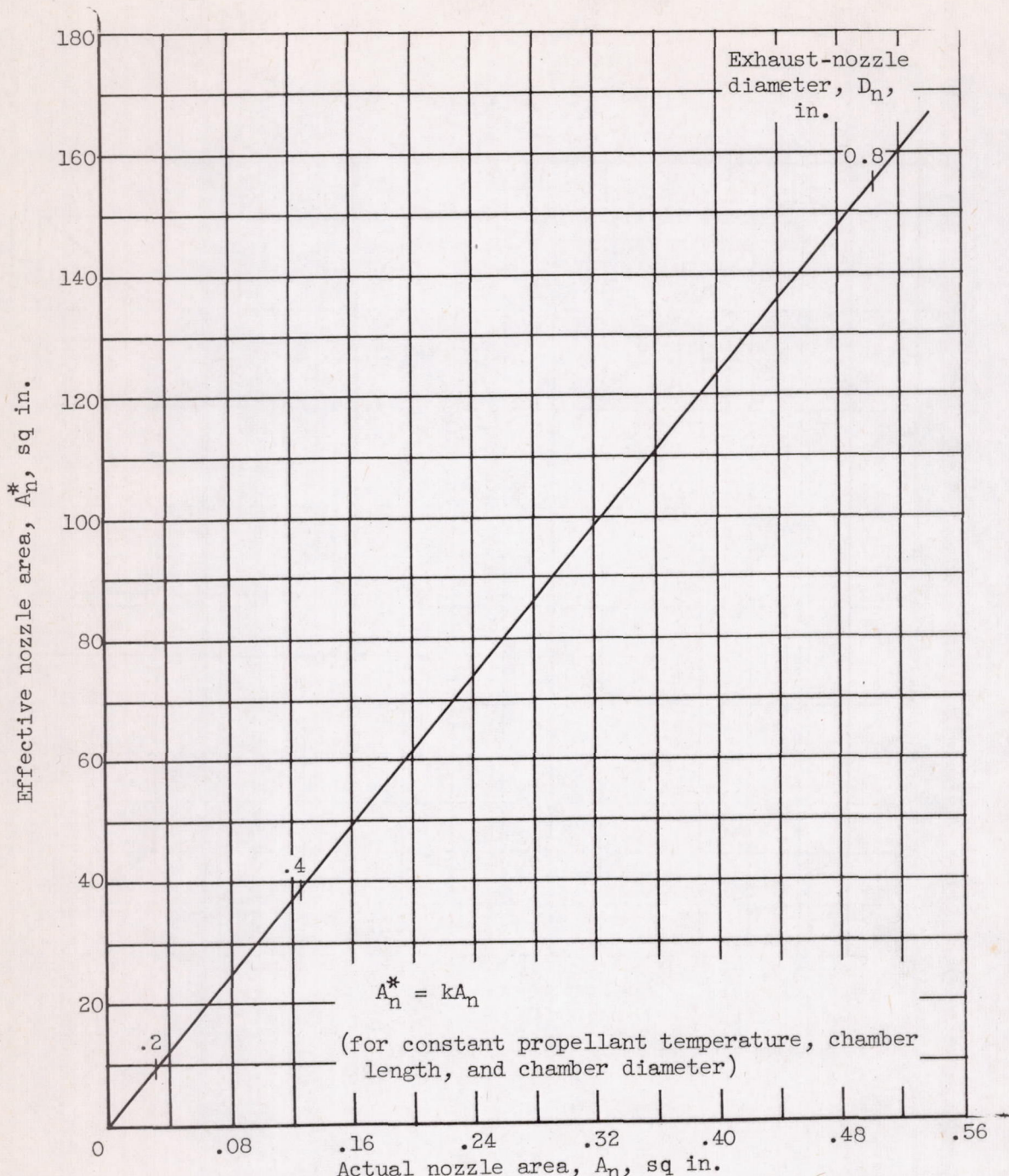


Figure 16. - Relation between effective and actual nozzle areas.  
 Propellant temperature,  $-90^\circ F$ ; chamber length, 1 inch; chamber diameter, 1 inch.

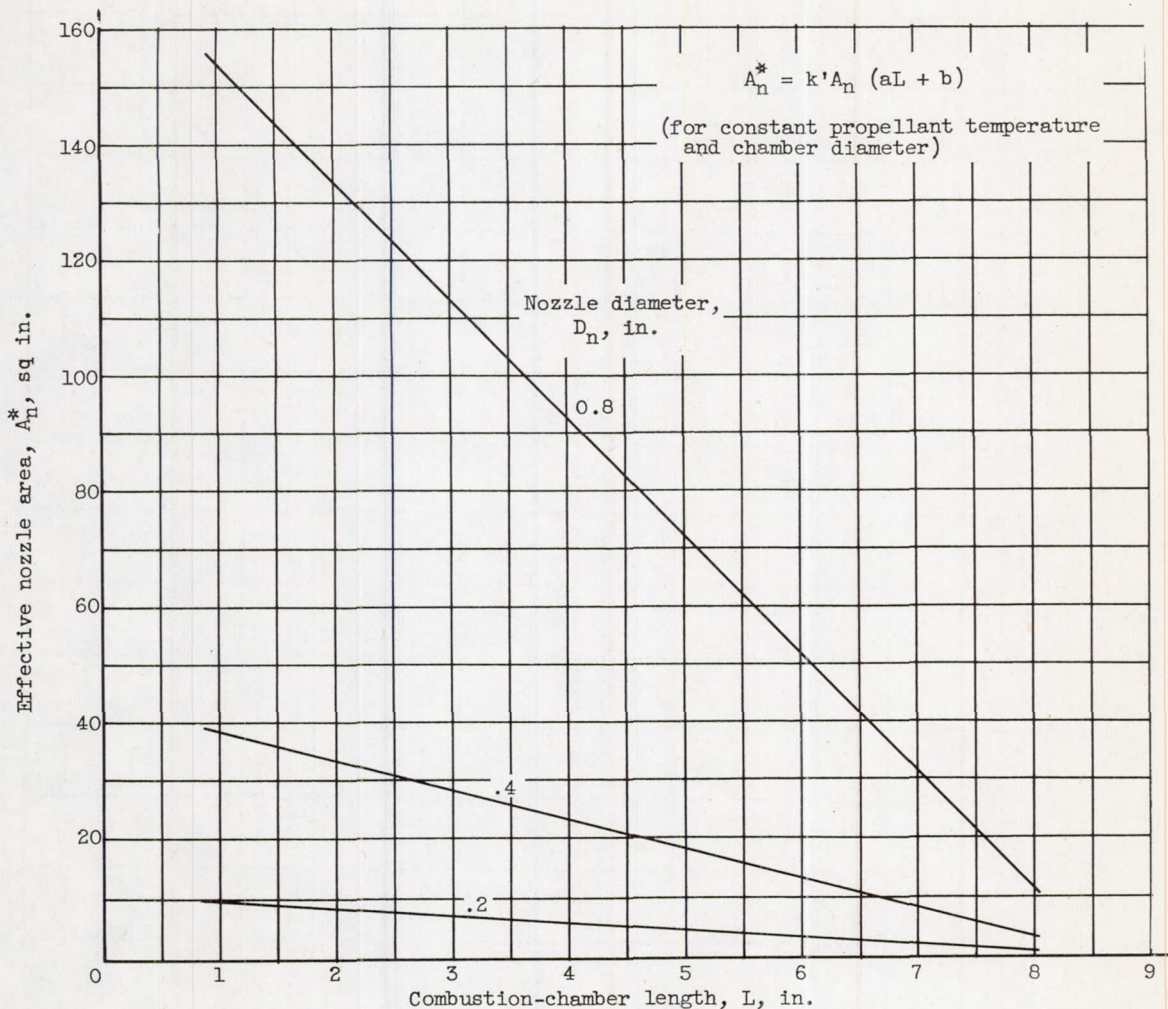


Figure 17. - Relation between effective nozzle area and chamber length (propellant temperature,  $-90^\circ$  F; chamber diameter, 1 in.).